Laboratory of Polymer Chemistry
Department of Chemistry
University of Helsinki
Helsinki, Finland

ADJUSTING THE PROPERTIES OF PNIPAM MICRO AND MACROGELS

Mirja Andersson

ACADEMIC DISSERTATION
FOR THE DEGREE OF DOCTOR OF PHILOSOPHY

To be presented, with the permission of the Faculty of Science of the University of Helsinki, for public examination in Auditorium 110 of the Department of Chemistry,
on 28 February 2014, at 12 o'clock.

Helsinki 2014

Supervisors

Professor Sirkka Liisa Maunu
and
Professor Heikki Tenhu
Laboratory of Polymer Chemistry
Department of Chemistry
University of Helsinki
Finland

Opponent

Professor Bo Nyström
Department of Chemistry
University of Oslo
Norway

Reviewers

Anna-Kaisa Kontturi
D.Tech.,Docent, Laboratory Administrator
Department of Chemistry
School of Chemical Technology
Aalto University
Finland

&

Janne Raula
PhD, Docent, Senior Research Associate
Department of Applied Physics
School of Science
Aalto University
Finland

ISBN 978-952-10-9737-9 (pbk.)
ISBN 978-952-10-9738-6 (PDF)

Helsinki University Printing House
Helsinki 2014

ABSTRACT

In dilute aqueous solution poly(N-isopropylacrylamide), PNIPAM, chain undergoes a coil-to-globule transition at its lower critical solution temperature, LCST, of ca. 32 °C. PNIPAM is one of the most studied polymers for instance for temperature controlled drug release systems, because its LCST is so close to body temperature. However, applicability of PNIPAM as gel-actuators or as active surfaces depends on the self-assembling microstructures and their physical properties. In this study several types of polymers based on PNIPAM (linear, microgels, macrogels, core-shell particles) were prepared and characterised with several methods.

The first part of the research focused in developing a temperature controlled release system for a drug, isobutylmethylxanthine (IBMX), based on a PNIPAM system with tailored properties. It is concluded, that the prepared macroscopic PNIPAM -copolymer gels, with properties adjusted chemically by adding the aromatic esters groups (benzoates and cinnamates) to the structures, exhibited higher IBMX binding capacity than the unmodified PNIPAM gel in pure water above the LCST. The release rates of IBMX from the gels are slowed down by the aromatic moieties in the polymer network. The binding of IBMX to the polymers is concluded to be due to both the specific complex formation between aromatic moieties and IBMX, and to hydrophobic interactions inside the hydrophobically modified PNIPAM.

In the second part of the research the structures of PNIPAM microgels synthesised with different concentrations of surfactant (SDS) and crosslinking monomer (MBA). Also PNIPAM microgels as shells on PS particles were studied. With high SDS concentrations during microgel synthesis, the precipitation of PNIPAM is prevented, and consequently tightly packed PNIPAM particle cores are not formed. In other words more homogeneously structured PNIPAM microgels are resulting. The concentration of MBA does not affect to the structure as dramatically as SDS, but the effect is clearly observed. Increasing hydrodynamic radius above the cloud point is observed with the increasing MBA concentration. This owes to the increasing size of the tightly crosslinked and rigid particle core. It is concluded that due to a relatively more rigid structure of the microgel at higher crosslinker concentrations, the volume phase transition broadens, and it is pushed towards higher temperatures. The enthalpy of transition is concluded to decrease with increased crosslinking density.

Phase transitions and structural characteristics of microgels were further studied with ^{1}H-NMR spectroscopy including the measurements of the signal intensities as well as the spin-lattice (T_1) and spin-spin (T_2) relaxation times

for the protons of PNIPAM with changing temperature. When analysing the relaxation times, the broad temperature range of study is divided in two parts, to cases above and below the LCST. When the suggested significant structural changes with the MBA concentration, and especially with the SDS concentration are taken into account, the results can be rationalised. In the homogeneous microgel structure also the charges should be more evenly distributed compared to the corresponding heterogeneous microgel structure with highly charged surface and insoluble core. As the zeta potentials are also suggesting, the negatively charged coronal layers (with high local LCST) in the heterogeneous microgels are likely to contribute to the proton signals well above the LCST.

According to the relaxation times from NMR-studies, it is concluded that there is more mobile structures of PNIPAM on PS core particles compared to the heterogenous microgel samples (a looser and/or more heterogeneous network structure). The results also show, that PNIPAM microgel shell on PS core inhibited the polymer–cell contact by steric repulsion similarly to PEO grafts, whereas PVCL coated PS was adsorbed on the cells more strongly, especially above the LCST. This result with a PNIPAM shell in the cell interaction study is in correlation with the observed high T_2 values referring to mobile components existing in 2-stage particle samples still above LCST, and supports the idea of local high LCSTs of coronal PNIPAM layers in the outermost parts.

ACKNOWLEDGEMENTS

The research described in this thesis was conducted in the Laboratory of Polymer Chemistry, Department of Chemistry, University of Helsinki, during the years 2000 - 2006. The work was financed through several research projects, and was supervised by Professors Heikki Tenhu and Sirkka-Liisa Maunu. The project funding during the early years for this research came through technology programs of TEKES (the Finnish Funding Agency for Technology and Innovation, the POTRA and DIAGNOSTICS 2000 - programs). Later on the work was funded by the University of Helsinki. The research financers, the supervising professors and co-authors of the original papers are gratefully acknowledged.

My parents gave me the wings. My husband showed me, how to fly. My daughter is the reason for landing safely.

This thesis i dedicate to the memory of my grandmother. Her strong, but tired wings were given rest last spring. Her life story is reminding me every day, that the challenges in my life are unique possibilities. Nowadays we can make choices and fullfill our dreams freely. Her generation is acknowledged for giving us that freedom.

CONTENTS

Abstract 3

Acknowledgements 5

Contents 6

List of original publications 8

Abbreviations and symbols 10

1 Introduction 12

1.1 Poly(N-isopropylacrylamide) 12

1.2 Literature review on aqueous PNIPAM gels with different structures 13

1.2.1 Microgels and macrogels 13

1.2.2 Structural studies on microgels 14

1.2.3 PNIPAM shell on solid particle core 16

1.2.4 Trends in the application oriented research 18

1.3 Aim and motivation of the study 19

2 Experimental part 23

2.1 Polymer syntheses 23

2.1.1 Macrogels (I) 23

2.1.2 Microgel particles (II-IV) 24

2.1.3 Microgel particles with PS core (II) 25

2.1.4 Microgel particles with fluorescent PS core (V) 26

2.2 Characterisation methods 28

2.2.1 Macrogels (I) 28

2.2.2 Particles (II-V) 29

3 Results and discussion 31

3.1 Macrogels: Interactions with IBMX (I) 31

3.1.1 Drug binding and release 32

3.2 Microgel particles 36

3.2.1 Phase transition and colloidal properties of particles in H_2O (II-IV) 36

3.2.2 Thermodynamic parameters of volume phase transition in H_2O (III, IV) 42

3.2.3 Volume phase transition observed from the NMR signal intensities in D_2O (II-IV) 45

3.2.4 Dynamic behaviour of polymer segments from the NMR relaxation times (II-IV) 48

3.3 Microgel particles with PS core (II) 53

3.3.1 Phase transition and colloidal properties of particles in H_2O 53

3.3.2 Thermodynamic parameters of volume phase transition in H_2O 56

3.3.3 Volume phase transition observed from the NMR signal intensities in D_2O 57

3.3.4 Dynamic behaviour of polymer segments from the NMR relaxation times 58

3.4 Fluorescent particles in application studies 60

3.3.1 Cell-polymer interactions of microgel particles with PS core (V) 60

4 Conclusions 61

References 64

LIST OF ORIGINAL PUBLICATIONS

This thesis is based on the following five (5) publications by the author, Mirja Andersson (previous last name Kivelä):

I Kivelä, M.; Tenhu, H.; Koskelainen, A. **Binding of 3-isobutyl-1-methylxanthine into copolymers of N-isopropylacrylamide**, European Journal of Pharmaceutical Sciences **2004**, 21, 607-616

II Andersson, M.; Hietala, S.; Tenhu, H.; Maunu, S. L. **Polystyrene latex particles coated with crosslinked poly(N-isopropylacrylamide)**, Colloid and Polymer Science **2006**, 284, 1255-1263

III Andersson, M.; Maunu, S. L. **Structural studies of poly(N-isopropylacrylamide) microgels: Effect of SDS surfactant concentration in the microgel synthesis**, Journal of Polymer Science Part B: Polymer Physics **2006**, 44/23 , 3305-3314

IV Andersson, M.; Maunu, S. L. **Volume phase transition and structure of poly(N-isopropylacrylamide)microgels studied with ^{1}H-NMR spectroscopy in D_2O**, Colloid and Polymer Science **2006**, 285, 293-303

V Vihola, H.; Marttila, A.-K.; Pakkanen, J. S.; Andersson, M.; Laukkanen, A.; Kaukonen, A. M.; Tenhu, H.; Hirvonen, J. **Cell-polymer interactions of fluorescent latex particles coated with thermosensitive poly(N-isopropylacrylamide) and poly(N-vinylcaprolactam) or grafted with poly(ethyleneoxide)-macromonomer,** International Journal of Pharmaceutics **2007**, 343:1-2, 238-246

The publications are referred to in the text by their roman numerals.

Contribution to papers I -IV: Author draw up the research plan and conducted the literature and experimental research. Author wrote the papers in collaboration with the co-authors.

Contribution to paper V: Author synthesised the coated fluorescent PS particles for the application studies (with the exception of the PVCL- coating on FPS core, that was synthesised by co-author A. Laukkanen). Author participated in writing the manuscript in collaboration with the co-authors.

Authors other contribution to research publications (referred to as VI, VII)

VI Huhtinen, P.; Kivelä, M.; Kuronen, O.; Hagren, V.; Takalo, H.; Tenhu, H.; Lövgren, T.; Härmä, H. **Synthesis, characterization, and application of Eu(III), Tb(III), Sm(III), and Dy(III) lanthanide chelate nanoparticle labels**, Analytical Chemistry **2005**, 77/8, 2643-2648

VII Huhtinen, P.; Kivelä, M.; Soukka, T.; Tenhu, H.; Lövgren, T.; Härmä, H. **Preparation, characterisation and application of europium(III) chelate -dyed polystyrene-acrylic acid nanoparticle labels**, Analytica Chimica Acta **2008**, 630:2, 211-216

Contribution to papers VI –VII: Author synthesised and characterised the polystyrene-based latex particles prior to the fluorescent-chelate labeling and the application studies. Author participated in writing the manuscript in collaboration with the co-authors.

ABBREVIATIONS AND SYMBOLS

^{1}H-NMR proton nuclear magnetic resonance
AA acrylic acid
AIBN α,α'-azoisobutyronitrile
Caco-2 intestinal cell lines
CEMA cinnamoyloxyethylmethacrylate
CMC critical micellisation concentration
D_2O deuterium oxide
ΔH_{cal} calorimetric enthalpy of transition
DLS dynamic light scattering
$\Delta T_{1/2}$ width of the transition at half-height
EGDM ethyleneglycol dimethacrylate
FDMA fluorescein dimethacrylate
FPS fluorescent polystyrene particles
FTIR fourier transformation infrared
HS DSC high sensitivity differential scanning calorimetry
H_2O water
IBMX isobutylmethylxanthine
KPS potassiumpersulphate
LCST Lower critical solution temperature
M_∞ total mass released at equilibrium
$MAC_{11}EO_{42}$ amphiphilic PEO-macromonomer
MBA N,N-methylenebisacrylamide
M_p mass of dry polymer
M_s mass of swollen polymer
M_t mass released at time t
NIPAM N-isopropylacrylamide
NMR nuclear magnetic resonance
PEO poly(ethylene oxide)
PS polystyrene
PVCL poly(N-vinylcaprolactam)
RAW264.7 macrophages
R_h hydrodynamic radius
SDS sodium dodecylsulphate
SR swelling ratio
T_1 spin-lattice relaxation time
T_2 spin-spin relaxation time
T_{max} temperature of the maximum heat capacity
T_{onset} onset temperature of the DSC endotherm
UV/VIS ultraviolet/visible
VBZ vinylbenzoate
VCL N-vinylcaprolactam

ζ zeta potential

1 INTRODUCTION

1.1 POLY(N-ISOPROPYLACRYLAMIDE)

The temperature-induced phase transition and the phase diagram of poly(N-isopropylacrylamide), PNIPAM, in water, first reported by Heskins and Guillet in 1968[1], has been an inspiration to an enormous amount of scientific research as well as to many suggestions of application during the recent decades. In a dilute aqueous solution PNIPAM chain undergoes a coil-to-globule transition at its lower critical solution temperature, LCST, of ca. 32 °C, as water molecules bound to the polymer chains are released.[2] It has been explained, that the polymer changes to hydrophobic as the temperature is raised above the LCST.[3] Although the solution properties of the polymer are already thoroughly investigated, there still appears to be concept clarifications in need, since Robert Pelton quite recently stated that the PNIPAM is never hydrophobic.[4] Aqueous PNIPAM gels, either microscopic or macroscopic, often also referred to as PNIPAM hydrogels, exhibit typically a sharp and large change of gel volume upon heating owing to the coil-to-globule transition of PNIPAM chains within the network structure.

Thermoresponsive polymers have been over the years considered as potential candidates to many applications relying on ”smartness” or ”intelligence”.[5,6] As the solution properties of linear PNIPAM and crosslinked gels swollen by water have already thoroughly been investigated since the sixties and the seventies, the current academic research interest on solution properties has shifted to other responsive polymers. More sophisticated and controlled PNIPAM nanostructures can currently be synthesised and characterised.[7-9] As the properties of aqueous linear PNIPAM are well-known and the chemical composition as well as the self-assembled colloidal structures can be controlled, we will see during the years to come the evolution of novel nanoparticle applications. Also the understanding of PNIPAM microgel properties of physical and structural origin is finally reaching the required level for controlled applications of the particles.[10-14]

The research work summarised in this thesis has contributed to the structural studies of PNIPAM microgel containing particles, their surface properties and to the methods applicable in such studies, especially by applying the NMR spectroscopy above and below the LCST in the combination of other characterisation methods. In this chapter the research literature on aqueous PNIPAM gel structures is reviewed as well as the trends in the application oriented research, relevant to the thesis topic.

1.2 LITERATURE REVIEW ON AQUEOUS PNIPAM GELS WITH DIFFERENT STRUCTURES

1.2.1 MACROGELS AND MICROGELS

A thorough general review on syntheses and on properties of various PNIPAM structures, including also macro- and microgels along with the linear polymer, was written by Schild in 1992.[2] The volume phase transition phenomenon of responsive macrogels was experimentally observed already 35 years ago by Tanaka.[15,16] The pioneers in the research on the volume phase transition phenomena of responsive macrogels, Tanaka and Hirotsu[17], contributed with their reviews in the following year. During the nineties the PNIPAM polymers and gels with numerous chemical variations as well as their intelligent applications in several fields created a wide research-platform including the controlled drug release systems.[6]

The preparation of thermoresponsive colloidal particles, commonly referred also as microgels, was pioneered by Pelton and coworkers in the case of N-isopropylacrylamide, NIPAM.[18] Aqueous and colloidally stable PNIPAM microgel particles showed, as the macrogels before them, a rapid volume phase transition upon heating above the LCST. The important developments in the area of thermoresponsive aqueous microgels were reviewed[19], and later the unresolved issues in the preparation and characterisation of PNIPAM microgels were reviewed and highlighted[20] by Pelton. Among the unresolved issues were mentioned the problems very familiar to all those who worked with the preparation of aqueous PNIPAM microgel particles, such as purification from soluble impurities (surfactants, linear/branched polymer fraction etc.), production of very small-sized colloidally stable microgels, and the understanding and control of the internal structure of the microgels. The issue of internal structure concerns the microgels prepared by batch copolymerisations of NIPAM and a crosslinking monomer, N,N-methylenebisacrylamide (MBA), in the presence of a small amount of surfactant or in surfactant-free conditions in water. In aqueous systems particle production from NIPAM has been shown to proceed via a precipitation polymerisation mechanism. The reaction is conducted above the phase separation temperature and in the presence of MBA. MBA is consumed more rapidly than NIPAM in the polymerisation, inducing the production of particles with heterogeneous internal structure due to non-uniform distribution of crosslinks in the radial direction.[21] PNIPAM macrogels, on the contrary, have been traditionally prepared under good-solvent conditions (in cold water or in organic solvents).[2] The approach results most likely in more homogeneous structure since the precipitation of PNIPAM particles is not affecting the distribution of crosslinks within the gels, as in the microgel-syntheses described.[18,21] The crosslinking monomer,

MBA, has been used frequently in the PNIPAM macro- and microgel syntheses due to its chemical similarity to the main monomer. Other crosslinking monomers have also been used, such as ethyleneglycol dimethacrylate (EDGM), especially when organic solvent is used as a reaction medium, and MBA has limited solubility.

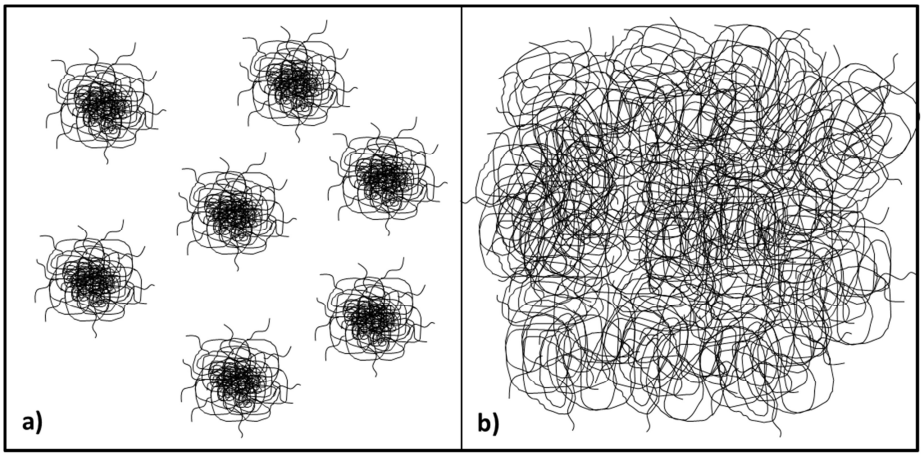

Figure 1. A representation of **a)** a microgel system (separate microparticles dispersed in a solvent phase) and **b)** a macrogel system (crosslinked polymer swollen by a solvent).

.

1.2.2 STRUCTURAL STUDIES ON MICROGELS

Several authors have discussed the internal structure of PNIPAM microgels. Most experimental studies have been based on scattering methods such as dynamic and static light scattering (LS), small-angle neutron scattering (SANS) and/or small-angle X-ray scattering (SAXS) to the structural characterisation of PNIPAM microgels, and plenty of evidence was provided on the heterogeneity of the internal structures.[22-26] Preparation of a homogeneous (uniform radial crosslinker density) microgel structure was reported by L. Arleth and coworkers in 2005. The PNIPAM microgel, synthesised as the heterogeneous ones but in the presence of high SDS concentration using MBA as the crosslinking monomer, was studied with SANS measurements, and a homogeneous structure was observed below and above the phase transition temperature.[27]

Woodward and coworkers investigated the volume phase transition of colloidal PNIPAM microgels prepared with varying crosslinker concentrations (0.25-30 % of MBA in monomer mixture) by surfactant-free

emulsion polymerisation.[28] In this case the system varies from a loose PNIPAM-network to a more compact and rigid particle structure with increasing crosslinking density. DSC analyses of these aqueous microgel particles showed that the T_{max} (temperature of the maximum heat capacity from the calorimetric endotherm) and the width of the volume phase transition increase with increasing crosslinker concentration. For example, T_{max} of the calorimetric endotherm increased by about 2°C when the amount of MBA in the monomer mixture was increased from 0.5% to 5%. The calorimetric enthalpy change of the transition decreased with increasing crosslinker concentration. The increased temperature of transition could indicate increased stability of PNIPAM in aqueous solution. However, the polarity of the interior of the microgels was studied with fluorescence spectroscopy by using pyrene as a probe. The results indicated that the hydrophobicity sensed by the probe increased with increasing crosslinker concentration. The calorimetric results were explained as being due to a relatively more rigid structure of the microgel at higher crosslinker concentrations, as a result of increasing rigidity the volume phase transition broadens and it is pushed towards higher temperatures.

Wu and coworkers studied the effect of MBA concentration on the swelling ability of PNIPAM microgels.[21] MBA has higher reactivity in radical polymerisation compared to NIPAM. It is assumed that there is a concentration gradient of the crosslinker in these microgels and the crosslinking density is decreasing from the particle core towards the surface. Similar conclusion was reached by Guillermo and coworkers when studying the heterogeneous structures of thermosensitive microgels of poly(N-isopropylmethacrylamide) produced with MBA[29] Assuming the existence of a core-shell-like structure, it was suggested that the relative size of the rigid core is increased upon increasing crosslinker concentration. This type of microgel particles are heterogeneous systems in which the crosslinking density determines whether the response to temperature is dominated by the phase transition of linear parts in the system or the volume phase transition of the gel structure.

PNIPAM microgels with various crosslinking densities (0.7-11 mol% of the monomers in the synthesis) have been studied also by Kratz and coworkers. They used several characterisation methods such as DLS, SANS, electron (EM) and atomic force microscopy (AFM).[23] The swelling ratio was observed to decrease with increasing MBA concentration, which was attributed to the topological constraints introduced through an increasing number of crosslinking points. It was concluded from their SANS data, that the polymer network in the swollen state becomes more heterogeneous with increasing crosslinker concentration. Interestingly, based on the swelling behaviour as function of temperature, it was concluded, that the transition temperature does not change significantly with crosslinker concentration,

and it was claimed that the thermodynamics of the process is not affected by the crosslinker density. The transition temperatures in their case were given by the inflection points of the derivatives of the deswelling curves: R_h (at temperature x) / R_h (in the swollen state at 15°C) versus temperature. However, broadening of the transition with increasing crosslinker concentration was observed.[23] The transition broadening and the decrease of swelling ratio with increasing crosslinking density were also observed in a light scattering study by Varga and coworkers.[22] They prepared the microgels based on the recipies of Wu et al.[21] in low SDS concentration (< 1 mM) and with varying MBA concentrations (<10 mol% of the monomers in synthesis). The structure of the microgel particles was found to strongly depend on the degree of crosslinking. In the swollen state the mean polymer density inside the microgel increased significantly with the crosslinker concentration, while in the collapsed state only a slight increase could be observed. They suggested that with increasing amount of the crosslinker the size of a strongly crosslinked core increases and the structure of the microgel particles gradually shifts from a loose network/highly branched polymer with a coil-like nature observed with DLS to a compact gel particle possessing a nonuniform segment density distribution inside and possessing a surface layer with very low crosslink density.[21,22]

1.2.3 PNIPAM SHELL ON SOLID PARTICLE CORE

Zhu and Napper pioneered the experimental studies on coil-to-globule transitions of linear PNIPAM chains attached to the surfaces of polystyrene latex particles. The kinetics of the transition was investigated in the case of chains grafted on polystyrene particles of ca. 100 nm in diameter by DLS and ^{13}C NMR spectroscopy.[30,31] Studies showed broadening of transitions of interfacial chains compared to free chains in solution. Further a considerable change in the coil-to-globule transition of interfacial chains was observed as the molecular weight (M_w) of the attached chains was varied from $3 * 10^5$ to $2 * 10^6$ g/mol. The broadening of the transition towards lower temperatures was more pronounced with the shortest polymer chains in question. The broad overall transition of the interfacial chains was explained to consist of two components. Upon heating, first the inner region of each chain adopts its globular form whereas the segments of chains in the coronal layer exist in the coil-like conformation until the LCST is reached.

There are interesting results reported also for PNIPAM on other solid particle surfaces. The phase transition of low molecular weight PNIPAM (ca. 5000 g/mol) covalently bound to the surface of gold clusters of few nm in size have been investigated with microcalorimetry by Shan and coworkers.[32] The PNIPAM chains in these monolayer protected gold clusters exhibited

two separate transition endotherms of dehydration around the LCST. The first transition with a sharp and narrow endothermic peak was observed at lower temperature while the second one with broader peak was observed at higher temperature. As in the case of Zhu and Napper it was suggested that the inner segments of chains close to the particle surface are densely packed and less hydrated showing the first transition while the segments in the coronal layer are more hydrated showing the second transition. As methods sensitive to dynamic properties in the phase transition on molecular level, both microcalorimetry and NMR spectroscopy have been employed to investigate the high molecular weight ($3.5 * 10^5$ g/mol) PNIPAM adsorbed on silica particles.[33] In this case the effect of the solid surface was an increased transition temperature and a broadening of the transition. Both effects were more pronounced at low surface coverage. The increase of the transition temperature was concluded to be due to increased motional constraints of the chains on the solid surface. The increase of the transition width was explained by the assumption of motional heterogeneity in the PNIPAM layer. At lower surface coverage the system is dominated by immobile segments close to silica while at higher coverage more mobile segments with a smaller broadening of the transition contribute. The studies of phase transition showed that PNIPAM chains on solid particles exhibits very different and more complex dynamic properties compared to volume systems in microgels.

Ballauff and coworkers[5,26,34-37] have studied the phase transition of PNIPAM microgel as a shell on a polystyrene based core. They prepared the core particles by conventional emulsion polymerisation of styrene and NIPAM (95/5 wt%) and as a second step they copolymerised NIPAM with the crosslinking monomer, MBA, in the presence of the core particles[34,35]. Phase behaviour of the thermosensitive shell in aqueous particle dispersions was studied by combining the data from different scattering methods such as dynamic light scattering (DLS)[35], small-angle neutron scattering (SANS)[26,36] and small-angle X-ray scattering (SAXS)[26,34]. The effect of temperature on the rheological properties of the particle dispersions was also studied[37]. Typically the core particles in aqueous dispersion were of approximately 100 nm in diameter and the crosslinked PNIPAM shell was of 10-50 nm in thickness depending on the temperature. It was shown that the PNIPAM shell in swollen state exhibited static and dynamic inhomogeneities, but clear evidences of radial distribution of crosslinks or inhomogeneities in the network were not found. Investigations by DLS revealed that a small number of chains extended beyond the network yielding a hairy surface. The volume phase transition of the shell was found to be continuous and the degree of shrinking was found to be much less than what is observed for macroscopic networks of a similar degree of crosslinking. This was suggested to be due to the fact that macroscopic networks shrink along three directions whereas the shell networks on a rigid core can only shrink in the dimension along the surface normal.

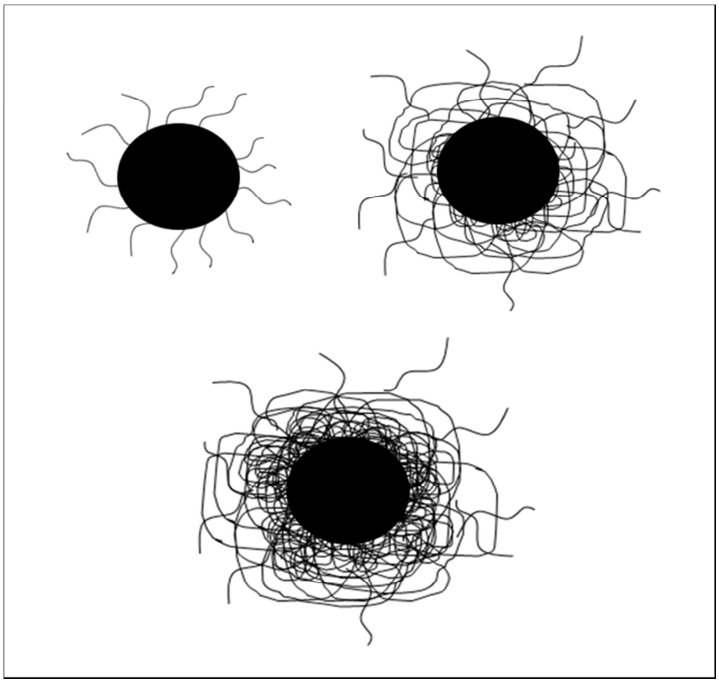

Figure 2. A representation of possible PNIPAM shell structures (adsorbed/attached linear chains or crosslinked networks) on solid particle cores, according to the reviewed literature.

1.2.4 TRENDS IN THE APPLICATION ORIENTED RESEARCH

The properties of aqueous PNIPAM systems most often utilised in applications, are the change of volume and the change of the interaction forces exerted to other molecules around the LCST. Traditionally PNIPAM has been one of the most studied polymers for temperature controlled drug release systems[6,38-41], in which both the volume change and the polymer – drug interactions are tailored for each purpose. In addition, crosslinked polymer networks swollen by water, serve as simple experimental tools to study the binding of low molar mass substances, such as drug molecules, into the polymers. In earlier studies on PNIPAM hydrogels conducted in our laboratory it was observed that binding of hydrophobic ibuprofen caused a considerable decrease in the swelling ratio below LCST whereas hydrophilic ephedrine did not have any effect.[42] Currently, with the developed knowledge and analysis tools, it is possible to study the drug –polymer- interactions on the molecular level within the PNIPAM gel structures using for example

high-sensitivity microcalorimetry and 1H-NMR- spectroscopy.[43] Similarly the developed knowledge of controlling the intern of PNIPAM microgels as well as the control of their surface properties is yielding new possibilities also for controlled drug release applications in nanoscale.[12-14]

The application oriented research interest currently lies on the surface properties and the molecular interactions of PNIPAM in nanoscale systems[44-46] instead of the gel volume change. The research on PNIPAM - microgel surfaces on solid core particles have given valuable information also for applications, where the surface behaviour of PNIPAM has to be controlled above and below the LCST.[5] Recently Li and coworkers[45] reviewed the numerous variation possibilities of amphiphilic core-shell particles, both from synthetic strategy and application point of view. The nano-size and the resulting large surface area with tailorability of the core chemistry and properties, but also the surface properties make them potential for applications in many fields requiring functional particles. Cole et al.[44] reviewed the application based research on PNIPAM surfaces interacting with proteins and cells above and below the LCST. They presented a principle model for a thermosensitive protein and cell attachment to the polymer surface. According to the model, there are adsorptive forces dominant towards proteins above the LCST whereas repulsion dominates below the LCST.

1.3 AIM AND MOTIVATION OF THE STUDY

The research reported in paper I (published in 2004) was financed by TEKES in the POTRA- technology program (POTRA - Polymers for building the future 2000-2003). Together with a collaborating research group in the Laboratory of Medical Technology, Helsinki University of Technology, we were interested in developing a PNIPAM based temperature controlled release system for xanthines, especially for isobutylmethylxanthine, IBMX. Koskelainen et al.[47] studied photoresponses of retinal rod cells. The light-induced electrical responses of vertebrate photoreceptors can be recorded even from cells in vivo. In the phototransduction cascade of vertebrate photoreceptor cells, the photoreceptor specific G-protein mediates between visual pigment and cyclic GMP phosphodiesterase.[48] In these studies of photoresponse kinetics by Koskelainen, IBMX was used as phoshodiesterase inhibiting compound to alter the phototransduction cascade. With proper calibration, photoreceptor cells in vivo can be used as biosensor in measuring concentration of phosphodiesterase inhibiting compound on retina. In the reseach of photoresponse kinetics, a temperature controlled release system for IBMX based on microgel particles, applied as suspension on retina would

be beneficial. If the drug binding and release properties of polymer matrix can be influenced and controlled by temperature, then it may be possible to obtain desired drug level in the application where it is not possible to give required drug solution injections without disturbing the system. Several xanthines, including 3-isobutyl-1-methylxanthine, cause tracheal relaxation and thus have antiasthmatic potential. This is considered to be the result of xanthines acting as phosphodiesterase inhibitors.[49] Theophylline is commonly used as bronchodilator, and it is also used as hydrophilic model drug in testing of release properties of pharmaceutical formulations and their matrix polymers.[50-56] Methylxanthines such as caffeine and theophylline are well known central nervous system stimulants. High doses of these xanthines cause central nervous system hyperexcitability and can cause epileptic symptoms.[57]

The purpose of the work reported in paper I was the binding of IBMX into copolymers and find out if temperature has any effect on the binding. On one hand, it was assumed that upon the thermal collapse of PNIPAM the IBMX molecules are squeezed out to the surrounding aqueous phase during dehydration of the polymer. On the other hand, if hydrophobic binding of IBMX is strong enough, the drug may remain in the polymer during and after the collapse. In either case, by altering temperature and ionic strength it should be possible to bind and release IBMX. The effect of ionic strength was not studied, but the effect of temperature on the binding of IBMX to linear copolymers was studied in aqueous solutions by dynamic light scattering and viscosimetry. The synthesised crosslinked polymers were studied by swelling and by IBMX binding and release tests to find out if IBMX binding can be increased by introducing aromatic ester groups into PNIPAM network. With encouraging results of this study the next step would be the syntheses of microgel particles of similar chemistry, and their testing in temperature controlled release of IBMX on retina. Corresponding colloidal microgels were prepared and preliminarily tested for the application in physiological salt solution. (This experimental data was not published.) It was noticed that the ionic strength should have been taken into account in the release tests with macroscopic gels since the drug molecules were released from the microgels instantly and uncontrollably. The question arose if the IBMX binding and release properties of macroscopic gels and colloidally stable microgels of similar chemical nature can be correlated, since the ionic strength has most likely significant influence on colloidal stabilisation of microgels as well as on the thermal responses of PNIPAM in both cases. Consequently, the interest grew to study PNIPAM microgel structures more closely.

The studies reported in papers II-IV (published in 2006) contribute to the discussion of the structural effects to the phase transition of aqueous PNIPAM microgel systems. In paper II PNIPAM based microgel shells were prepared onto solid polystyrene latex particles. Phase behaviour of the

synthesised PNIPAM shells was studied in comparison with the traditional, heterogeneous (non-uniform radial crosslinker density), PNIPAM microgels.[21]The earlier studies by Ballauf and coworkers[26,34-37] had shown that, PS core has significant effects to the phase behaviour of PNIPAM-microgel shell. The aim of the study, reported in paper II, was to obtain new information on similar structures by applying especially liquid state ^{1}H NMR and microcalorimetry to follow the phase transition. The microgel research reported in papers III-IV was especially inspired by the results of Arleth and coworkers. Preparation of a homogeneous (uniform radial crosslinker density) microgel structure was reported by this group in 2005. The PNIPAM microgel, synthesised as the heterogeneous ones but in the presence of high SDS concentration using MBA as the crosslinking monomer, was studied with SANS measurements, and a homogeneous structure was observed below and above the phase transition temperature.[27] In paper III the aim was to study the structures of PNIPAM microgels synthesised in different concentrations of SDS, by measuring temperature dependences of both the ^{1}H NMR spectra and the ^{1}H NMR relaxations of PNIPAM microgels. In addition, microcalorimetry, turbidometry, dynamic light scattering (DLS) and electrophoretic mobility measurements were used to characterise the aqueous microgels at different temperatures.

In paper IV the aim of was to study the structures of PNIPAM microgels synthesised with different concentrations of the crosslinking monomer, MBA, in the presence of both small and large amount of surfactant, SDS, correspondingly. Guillermo and coworkers studied heterogeneous structures of corresponding thermoresponsive microgels of an another poly(acrylamide) derivative, poly(N-isopropylmethacrylamide), by liquid state ^{1}H NMR with relaxation measurements at room temperature.[29] At the time, there were only few reports of applying the liquid state NMR in the studies of the physical structure of PNIPAM microgels. Solvent diffusion measurements at various temperatures by the PGSE (pulsed-gradient spin-echo) NMR had been reported, and later the same approach was used to study the effect of the crosslink density on the volume phase transition of PNIPAM microgels.[28,58] Even in the basic case of linear PNIPAM homopolymer the applications of ^{1}H NMR spectroscopy to investigate the phase transition were rather seldom[58-63] Spevacek and coworkers have done systematic work to study the phase separation of other thermoresponsive polymers [64-70] and also linear PNIPAM [69] in D_2O by measuring temperature dependences of the ^{1}H NMR spectra and the ^{1}H NMR relaxations. The lack of better knowledge on PNIPAM microgels was considered a problem, and simply more information on the temperature dependence of the ^{1}H NMR spectra and the ^{1}H NMR relaxations of PNIPAM microgels was needed. The influence of the MBA-crosslinker concentration in the microgels prepared in zero/low SDS concentrations had been studied mainly by other methods.[22,23,71-76] Some years after the papers II-IV, the use of NMR methods

for studying of PNIPAM systems with various aims in aqueous media was reviewed 2009 by Spevacek.[70] Generally it was stated, that NMR methods provide several promising tools for the research of the structure and interactions of PNIPAM in complex systems with various architectures. The full potential of NMR methods is not yet utilised.

The cell–polymer interactions of thermosensitive poly(N-isopropylacrylamide) (PNIPAM) or poly(N-vinylcaprolactam) (PVCL) coated particles with RAW264.7 macrophages and intestinal Caco-2 cells were evaluated in paper V (published in 2007). Particles were prepared by modifying the surface of fluorescent polystyrene (FPS) particles with the thermosensitive polymer gels or with poly(ethylene oxide) (PEO) macromonomer grafts. Effects of temperature and polymer coating/grafting on the cellular interactions were evaluated by cell association/uptake and visualized by confocal scanning microscope.

2 EXPERIMENTAL PART

2.1 POLYMER SYNTHESES

In all cases polymers were prepared by free radical co-polymerisation of the monomers in an elevated temperature and using an external initiator compound producing radicals upon heating. Macrogels were prepared in an organic solvent and microgel particles in aqueous system. The numerous recipes for macrogels (for example ref. 2) reported earlier were applied for the study summarised here (paper I). PNIPAM –based, hydrophobically modified, macrogels were prepared for a model drug (IBMX) binding and release experiments described in this thesis.

The recipes reported by Wu et al.[21] were applied in the preparation of the PNIPAM microgel samples (papers II-IV) described in this thesis. Microgel syntheses were however adjusted by varying the surfactant (SDS) and the crosslinking –monomer (MBA) concentrations to study the structural changes. In the syntheses of the microgel particles with polystyrene core the procedures earlier reported by Ballauf and coworkers were applied.[34,35] Details of the used materials are given in the original papers. All the syntheses of the polymers discussed in this thesis are summarised below.

2.1.1 MACROGELS (I)

A comonomer, cinnamoyloxyethyl methacrylate (CEMA), was first synthesised by reacting 2-hydroxyethyl methacrylate with cinnamoyl chloride in dichloromethane. Triethylamine was used as a catalyst in esterification. The synthesis and purification of CEMA was conducted by following a procedure reported by Hyder Ali and Srinivasan.[77] The crosslinked polymers were prepared by radical polymerisation in dioxane at 70°C. The monomer ratios used in the syntheses and the abbreviations for the crosslinked polymers are summarised in Table 1. Monomers, the crosslinker (EDGM, 4 mol% of monomers) and the initiator (AIBN, 1 mol% of monomers) were dissolved in 8 ml dioxane in polypropylene test tubes with the diameter of 14 mm. The tubes were closed with a septum and the solutions were purged with nitrogen for 20 min. The tubes were then placed to an oil bath at 70°C. Polymerisation was carried out for 3 hrs after which the bottoms of the tubes were cut off and the cylindrical gels were carefully pushed out from the tubes. The gels were soaked in dioxane for a few days

and then cut to 0.5 cm thick slices. The disclike slices of N100, N98C2 and N95C5 were soaked in ethanol for a week to remove unreacted compounds, but in the cases of N80V20 and N90V10 acetone was used in purification instead of ethanol. In all cases the solvents were refreshed daily. The slices were dried for 24 hrs in air and in a vacuum desiccator for another 24 hrs.

Table 1. *The molar ratios of the main monomers used in the macrogel-syntheses. In addition, the crosslinking monomer, EGDMA, was used (4 mol% of the total amount of the main monomers), as well as the initiator, AIBN, (1 mol%).*

Sample code	N100	N98C2	N95C5	N90V10	N80V20
NIPAM	100	98	95	90	80
VBZ				10	20
CEMA		2	5		

2.1.2 MICROGEL PARTICLES (II-IV)

Polymerisations were carried out in a sealed round-bottom flask equipped with a magnetic stirrer and an oil bath to control the reaction temperature. In a typical synthesis NIPAM and MBA were separately dissolved in premade aqueous solution of SDS and both solutions were transferred into the reaction flask. The flask was sealed with a septum, and the solution was purged with nitrogen and stirred at room temperature for 20 minutes. The nitrogen inlet and outlet were removed and the flask was placed into a preheated oil bath at 70°C. Polymerisation was initiated after stirring (650 rpm) for 20 minutes by injecting KPS, dissolved in 2ml of water, to the reaction mixture. Total amount of water used in a polymerisation batch was typically 20-26 ml. The reaction was allowed to proceed in stirring for 4 hrs. The reaction was stopped by unsealing the flask and cooling the product to room temperature. The product was filtered through a filter paper. The aqueous microgels dispersions were purified by dialysis for 7 days against distilled water that was refreshed daily (twice during the first 3 days). The purified dispersions were stored as such in the refrigerator. Polymer contents of aqueous microgel dispersions were obtained by drying weighed samples of aqueous dispersions to equilibrium weight in vacuum. The molar concentrations of SDS and MBA in each synthesis batch are listed in the Table 2 as well as the sample coding. The respective amounts of NIPAM, initiator and water were kept constant. The M-coding refers the sample set were MBA concentration is the variable. The samples used to study the effect of SDS concentration were coded with S-codes.

Table 2. *Preparation and coding of the microgel samples. In the synthesis batches: NIPAM 130 mM, KPS 2 mM and water 20-26 ml (total amount).*Close correspondant to the traditional recipe (for example Wu and coworkers, ref. 21).*

Sample coding Papers III – IV	**MBA mM**	**SDS mM**
M1.6 / S0.4*	**1.6**	**0.4**
M3.2	**3.2**	0.4
M6.5	**6.5**	0.4
M13	**13**	0.4
S1.3	4.2	**1.3**
S4.0	4.2	**4.0**
M4.2S / S6.7	**4.2**	**6.7**
M6.5S	**6.5**	6.7
M8.4S	**8.4**	6.7
M13S	**13**	6.7

2.1.3 MICROGEL PARTICLES WITH PS CORE (II)

A summary of the conditions of the syntheses and the abbreviations for the particles are shown in Table 3. Polymerisations were carried out in a sealed round-bottom flask equipped with a magnetic stirrer and an oil bath to control the reaction temperature. The seed particles, PS1 and PS2 were prepared by radical polymerisation of styrene in aqueous emulsion. Surfactant, SDS, was dissolved in water in the reaction flask after which styrene was added and the flask was sealed with a septum. The mixture was purged with nitrogen and stirred at room temperature for 20 minutes. The nitrogen inlet and outlet were removed and the flask was placed into a preheated oil bath at 60°C. Polymerisation was initiated after 20 minutes by injecting KPS dissolved in 1ml of water to the reaction mixture after which reaction was allowed to proceed for 3 hrs with stirring (600-700 rpm). The reaction was stopped by unsealing the flask and cooling the product to room temperature. The product was filtered through a filter paper and purified by dialysing for 7 days against distilled water that was refreshed daily. The dialysed aqueous particle dispersion was extracted several times with n-hexane and stored as such in the refrigerator.

The two-stage particles were prepared by the following manner. In the synthesis of particle PS1N, NIPAM and MBA were separately dissolved in aqueous seed particle dispersion, PS1, and both solutions were transferred to a reaction flask. The flask was sealed with a septum and polymerisation was initiated and carried out by following the procedure described for the synthesis of seed particles. In the synthesis of particle PS1NA, acrylic acid was in addition injected to the reaction mixture before sealing the flask. For the synthesis of PS2N, the purified seed particle dispersion, PS2, was diluted with 12.5 ml of water prior to use in polymerisation. In the second stage polymerisations the reaction time was 20 hrs and the reaction temperature was 60°C. Particles were purified by dialysis for 7 days against distilled water that was refreshed daily. The purified particle dispersions were stored as such in the refrigerator. Polymer contents of aqueous particle dispersions were obtained by drying weighed samples of aqueous dispersions to equilibrium weight in vacuum.

Table 3. *Summary of the syntheses. (The components of the reaction mixtures are given as grams.)[a] PS1 particle dispersion (particle concentration 2.8 wt%); [b] PS2 particle dispersion (particle concentration 3.2 wt%)*

Particle	H_2O	Seed	SDS	KPS	Styrene	NIPAM	MBA	AA
PS1	30		0.3	0.06	2.25			
PS2	30		0.3	0.06	2.25			
PS1N		20[a]		0.01		0.2	0.013	
PS1NA		20[a]		0.01		0.2	0.013	0.004
PS2N	12.5	17.5[b]		0.015		0.3	0.02	
N1	20		0.002	0.01		0.3	0.02	
N2	50		0.005	0.03		0.75	0.025	

2.1.4 MICROGEL PARTICLES WITH FLUORESCENT PS CORE (V)

Fluorescent PS-particles with different surface coatings were prepared for the cell-polymer interaction studies with a collaborating research group in pharmaceutical technology. First fluorescent seed particles were prepared using styrene as a main monomer together with the fluorescent co-monomer, fluorescein dimethacrylate (FDMA). The fluorescent seed particles, FPS, were prepared by radical copolymerisation in an aqueous emulsion using SDS –surfactant and KPS –initiator with the procedure described for the seed particles PS1 and PS2 in the earlier chapter 2.1.3.

The PEO-macromonomer grafted particles, FPS-PEO, were prepared by dissolving KPS -initiator and the amphiphilic PEO- macromonomer ($MAC_{11}EO_{42}$), ω-methoxy poly(ethyleneoxide)$_{42}$ undecyl α-methacrylate, in water after which styrene and FDMA were added. The amphiphilic, non-ionic PEO-macromonomer, was prepared and characterised in our laboratory earlier with the procedure reported by Laukkanen et al.[78]

In the synthesis of FPS-PNIPAM, NIPAM and the crosslinking monomer (MBA) were separately dissolved in the aqueous FPS seed particle and the synthesis was carried out with the procedure described for the corresponding PNIPAM coated particles in the earlier chapter 2.1.3. FPS-PVCL was prepared similarly but using the vinylcaprolactam-monomer instead of NIPAM. All the polymerisation reactions were allowed to proceed at 70-80 °C for 3 hours with stirring and stopped by cooling. The products were filtered and purified by dialysis. The FPS seed particles were in addition to dialysis extracted with n-hexane. The purified particle dispersions were stored as such in the refrigerator. Polymer contents of aqueous particle dispersions were obtained by drying weighed samples of aqueous dispersions to equilibrium weight.

The detailed synthesis recipies for particle samples coded as FPS, FPS-PNIPAM, FPS-PEO and FPS-PVCL used in the study are reported in the original paper. The author of this thesis was responsible for all the particle syntheses with the exception of the coating of the FPS-seed with PVCL. Recipies are summarised in Table 4. The PVCL-coating was synthesised by co-author, A. Laukkanen.

Table 4. *Syntheses mixtures for the fluorescent particles.*

Sample	Water/seed Ml	Styrene mmol	FDMA mmol	NIPAM mmol	$MAC_{11}EO_{42}$ mmol	MBA mmol	KPS mmol	SDS mmol
FPS	10	7.7	0.043				0.074	0.347
FPS-PNIPAM	10 (FPS)			1.325		0.065	0.022	
FPS-PEO	10	6.2	0.043		0.136		0.148	

2.2 CHARACTERISATION METHODS

The main methods used in characterisation for obtaining the results discussed in this thesis are briefly listed here. Further information on details can be found in original papers.

2.2.1 MACROGELS (I)

For the swelling tests dry polymer discs were swollen in pure water and in aqueous solutions with varying IBMX concentrations. The samples were equilibrated in a thermostated water bath at temperatures ranging from 35 to 5°C. The gels were weighed at each temperature step. The swelling ratios of the gels were calculated as $SR = (M_s - M_p) / M_p$, where M_p is the mass of dry polymer and M_s is the mass of swollen polymer.

For the IBMX binding tests, dry polymer discs were placed in aqueous solutions of IBMX. The solutions were equilibrated at 35 and 21°C as in the case of swelling tests. At each temperature, small samples were taken from the solutions above the gels for IBMX concentration measurements. The IBMX concentrations were measured with a UV/VIS spectrophotometer (Shimadzu 160 1PC).

For the IBMX release tests, an exact amount of an ethanol solution of IBMX was added on dry gel. Ethanol was evaporated from the gels in vacuum for 24 hrs. The IBMX loaded polymer was dropped into a quartz cuvette containing 3.0 ml water at a fixed temperature. The absorbance measurement with a UV/VIS spectrophotometer was started immediately at 273 nm wavelength to obtain the concentration of IBMX released to the aqueous phase above the gel. The absorbance was recorded as a function of time for 300-360 min and the final absorbance was measured after 24 hrs, and checked after further 24 hrs to obtain the equilibrium release value. UV measurements were carried out at 21°C and 35°C. The results are given as a function of time in relative units M_t / M_∞ , where M_t is the mass of IBMX released at time t and M_∞ is the total mass of IBMX released at equilibrium.

2.2.2 PARTICLES (II-V)

The size distributions of particles were obtained with dynamic light scattering (DLS) by using the instrument of Bookhaven Instruments (BI-200SM goniometer, BI-9000AT digital correlator) equipped with LEXEL 85 1W laser at wavelength 514.5 or with an argon laser at 488 nm. Scattering was measured at 90° angle and the obtained time correlation functions were analysed by CONTIN Laplace-inversion program. Typically the polymer concentration in the light scattering sample was 0.01 mg/ml obtained by diluting the particle dispersion with deionised water. Temperature of the sample unit was controlled with Lauda RC6 CP-thermostate. (papers II-V)

HS DSC (High sensitivity differential scanning calorimetry) measurements were performed with a VP-DSC microcalorimeter (Microcal Inc.) at an external pressure of ca. 180 kPA. The cell volume was 0.507 ml. Scans were recorded from 10°C to 80°C at heating rates 30°C/h and 60°C/h. Prior to each scan the sample was kept at 10°C for 15 min and each scan was repeated 3 times. Data was analysed by using the software supplied by the manufacturer. The raw data from HS-DSC was corrected by subtracting the baseline, and with corrections to the sample concentration terms, where the sample concentration was given as molar concentration of NIPAM units in the particle sample. The samples were prepared from dialysed particle dispersions by diluting with deionised water. Also some samples prepared from freeze-dried particles were measured in H_2O and D_2O. Particle concentrations were of 2-20 g/l. (papers II-IV)

The zeta potentials of the aqueous microgel samples were measured using a zetapotential analyser (Malvern Zetasizer 3000HSA, Malvern Instruments) at temperatures 20°C and 40°C. Samples were prepared by redispersing freeze-dried microgels in deionised water. Polymer concentrations in aqueous dispersions used in the measurements were 0.1-1 g/l. Electrophoretic mobilities (depending on the sizes and charges of the analytes, and on the type of the solvent) of the microgels in aqueous dispersion were first measured and the zeta potentials, ζ , were calculated from the mobilities with the software supplied by the Zetasizer manufacturer using the Smoluchovski approximation of the Henry function. The Smoluchovski approximation gives the most accurate approximations of the zeta potentials in the cases where the particle sizes are > 100nm in aqueous solutions with ionic strengths > 10^{-3} M. (papers II-IV)

In turbidometric characterisation the change of optical density (absorbance) of the aqueous dispersions of the microgels was monitored at a wavelength of 500 nm with a UV-Vis spectrophotometer (Shimadzu 1601PC) as a function of temperature. The temperature of the sample unit was controlled with

Huber Ministat -thermostate programmed to heat at rate 12°C/h from 20°C to 50°C. The polymer concentrations in the samples were 1 g/l and the samples were prepared from freeze-dried polymers. (papers II-IV)

^{1}H NMR spectra and relaxation measurements of the particles in D_2O were measured using a Varian UNITYINOVA spectrometer operating at 300 MHz for protons equipped with a temperature control unit. The NMR samples were prepared by redispersing 20 mg of freeze-dried particles in 1 ml of D_2O and filtered through a filter paper. Measurements were carried out with controlled heating and cooling steps, allowing the samples to equilibrate for 30 min at each incremented temperature. For the ^{1}H T1 relaxation measurements of the polymer protons a series of ~30 spectra were collected using the standard inversion recovery sequence varying the delay time from 0.001 to 10 s. The ^{1}H T2 relaxation measurements of the polymer protons were made using the Carr-Purcell-Meiboom-Gill spin-echo sequence using an array of ~20 values ranging from 0.002 s to 1 s. The T1 and T2 relaxation times were obtained by fitting a monoexponential decay to the relaxation data. (papers II-IV)

3 RESULTS AND DISCUSSION

3.1 MACROGELS: INTERACTIONS WITH IBMX (I)

PNIPAM –based, hydrophobically modified, copolymers were prepared for a drug (IBMX) binding and release experiments described in this thesis. The syntheses are briefly described in chapter 2.1. (macrogels) and in more detail (macrogels and linear copolymers) in the original paper I. The chemical structures copolymers (excluding the crosslinking monomer used in macrogels) as well as the model drug are given in figure 3.

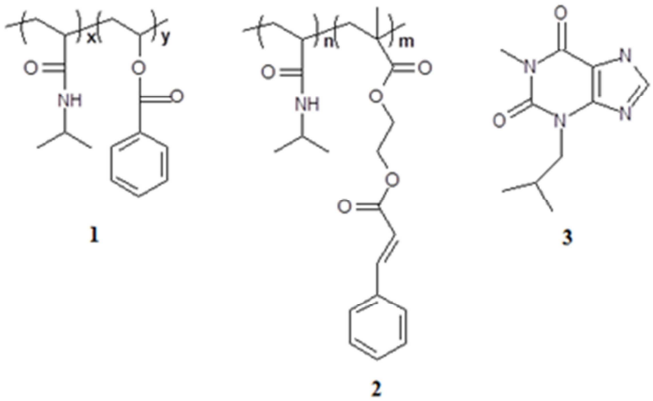

Figure 3. The structures of 1) poly(NIPAAm-co-vinyl benzoate), 2) poly(NIPAAm-co-cinnamoyloxyethyl methacrylate), and 3) IBMX

In designing of new polymeric materials for controlled drug release systems, the studies on the interactions between the polymers and the drug molecules are essential. Connors and coworkers studied the molecular complexes between xanthines and several aromatic esters such as cinnamates and benzoates in aqueous solutions.[79-82] It is suggested that these 1:1 complexes have a plane-to-plane orientation but the complex structures do not involve maximum overlap of π-orbitals. The classical electron donor-acceptor or charge-transfer interaction seems to be unlikely as the major source of the complex stability. Hydrophobic bonding may be important as well as local dipole-dipole attraction forces. The contribution of the solvent structure in stabilising complexes could be a significant factor. Xanthines

have also a tendency to self-associate in solutions.[83] The association in solutions is explained by plane-to-plane stacking of xanthine molecules with themselves or other xanthines. The stacking can be a co-operative result of hydrophobic interactions, hydrophilic hydration and possible polarizability effects.[84]

With this information vinyl benzoate (VBZ) and cinnamoyloxyethyl methacrylate (CEMA) were chosen to be copolymerised with NIPAM to tailor the drug-binding properties. The behaviour of the synthesised linear copolymers depended on the IBMX concentration in aqueous solutions above and below LCST, as observed by viscosimetry and dynamic light scattering. (Experiments described in detail in the original paper I.) The collapse of the copolymer coils and also increased aggregation was observed with certain molar ratios of IBMX to the aromatic units in the copolymer chain in the aqueous solutions. These results were in accordance with the assumed complex formation between the copolymers and IBMX that was suggested by the literature. After these promising results with the linear copolymers, crosslinked co-polymer gels were studied with IBMX binding and release tests as described next.

3.1.1 DRUG BINDING AND RELEASE

In this study, the IBMX binding experiments were conducted for each aqueous gel at 21 and 35°C. The results are shown in Figure 4 a. At 21°C, the hydrophobically modified gels N90V10 (V for vinyl benzoate) and N98C2 (C for cinnamoyloxyethyl methacrylate) bind less IBMX than the homopolymer gel, N100, but the increase of the amount of the aromatic comonomer in the polymer has a positive effect on binding capacity. The hydrophobically modified gels have smaller water uptake (swelling ratio, SR) than the homopolymer gel at this temperature. The swelling ratios for the gels in pure water and the relative swelling in aqueous solutions with varying IBMX concentrations at 21°C are listed in table 5. The reduction of the uptake of the IBMX solution decreases the possibilities of polymer to interact with IBMX during the experiment and so may decrease binding. Increased hydrophobicity of the modified gels is clearly observed by comparing the swelling ratios at At 35°C, in the shrunken state there is less variation in water uptake between the gels. All aromatic copolymer gels exhibit higher binding capacity than the homopolymer gel as shown in Figure 4 a.

Drug release behavior of swellable polymers can be analysed based on the empirically derived equation: $M_t / M = kt^n$, where k is the rate constant.[85] For drug release governed by diffusion, n is 0.5. The time dependent release

becomes zero-ordered (n=1) in certain swelling controlled systems. The time dependence of the fractional IBMX release from the gels during swelling at 21°C and at 35°C is presented in Figure 4 b. The hydrophobically modified gels with the lowest equilibrium swelling ratios, N95C5 and N80V20, are also the slowest releasers showing release profiles typical for diffusion controlled systems. However, N100, N92C2, and N90V10 swell more at this temperature and thus show higher release rates as the solute diffusitivity increases with an increase in the swelling ratio. As shown in the Figure 4 b, the homopolymer, N100, is the fastest releaser at 35°C. In the shrunken state, at 35°C, the effect of swelling on the release rates is minimal and the release is diffusion controlled. The copolymer gel, N95C5, exhibits nearly zero release of IBMX during the 6 hrs of the experiment. The equilibrium release from N95C5 is only 0.03 wt% of the loaded IBMX. At both 21°C and 35°C, the equilibrium release is decreased by the aromatic units in the polymer network.

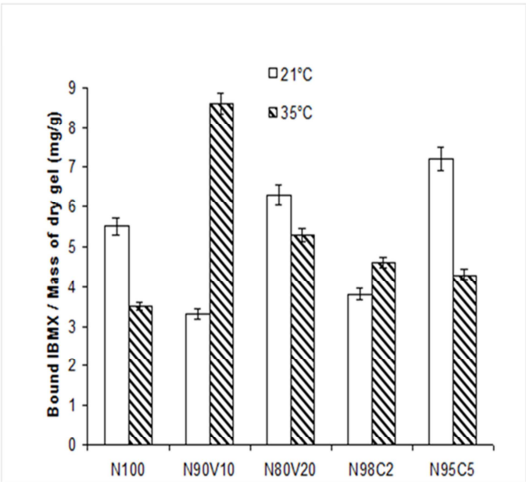

Sample	N100	N98C2	N95C5	N90V10	N80V20
Monomer			Molar ratios in feed (%)		
NIPAM	100	98	95	90	80
VBZ				10	20
CEMA		2	5		

Figure 4 a. The saturation binding of IBMX from aqueous solution (0.5 mg/ml) into initially dry gels below and above LCST. Sample coding is given in the table embedded in the figure (note that EGDM –crosslinker was used in addition, 4 mol%).

Table 5. *Swelling the macrogels in pure water and relative swelling in IBMX solutions.* [a]*Swelling ratios (SR) of the gels in pure water at various temperatures.* [b]*Relative swelling in aqueous solutions with varying IBMX concentrations at 21℃.*

Sample	N100	N98C2	N95C5	N90V10	N80V20
[a] Temperature					
5 (°C)	48.0	30.0	18.7	43.0	31.6
10	45.0	27.6	14.3	40.0	29.2
21	26.3	10.5	2.80	20.9	4.60
30	0.59	0.34	0.26	0.44	0.29
35	0.26	0.28	0.24	0.30	0.26
[b] [IBMX]					
0 (mg/ml)	1.00	1.00	1.00	1.00	1.00
0.2	0.99	0.99	0.92	0.95	0.88
0.3	0.98	1.02	0.92	0.99	0.94
0.4	0.98	0.99	0.88	0.96	0.87
0.5	0.97	1.02	0.81	0.97	0.85

Makino and coworkers studied drug release behavior of negatively charged PNIPAM hydrogel disks with anionic, cationic and non-ionic drug with an experimental method similar to the method used in this work with the exception of flowing water conditions.[86] As in our experiments, a lag phase was observed before the amount of drug released from initially dry polymer at fixed temperature within a range 25-40°C became proportional to time. Length of a lag phase was found dependant on both temperature and interactions between drug molecules and the polymer. With all the drugs the lag phase was longer at 35°C than at 25°C. In this study, the IBMX release data shows that the lag phase is longer for each gel at 35°C than at 21°C. The differences of the lag times between the gels are more pronounced at 35°C, even so that diffusion of IBMX from N95C5 is almost completely hindered.

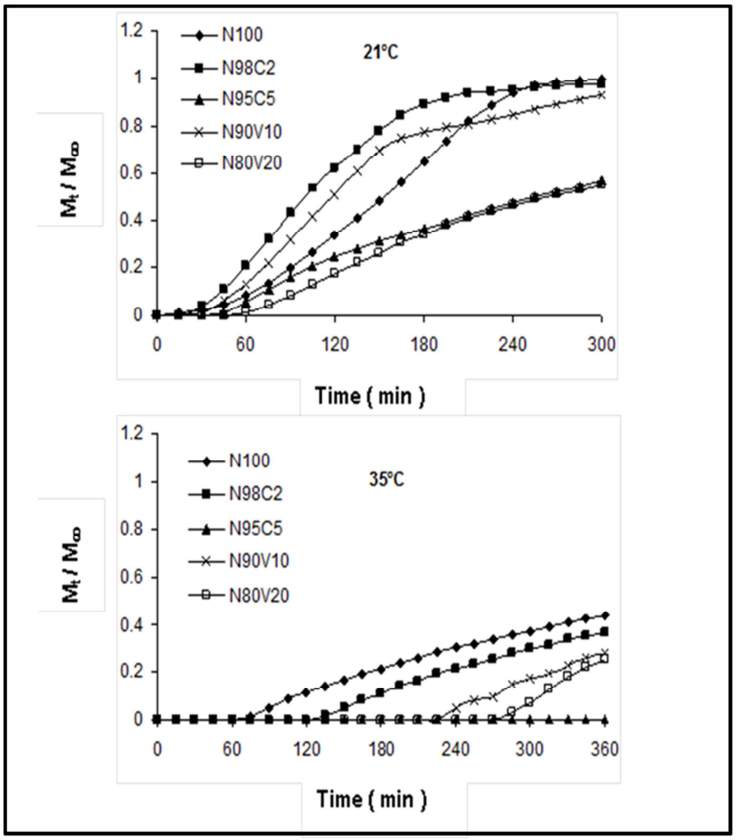

Figure 4 b. Time dependence of the fractional IBMX release from the gels (dry weights 2-3mg) during swelling at 21℃ and at 35℃. The amount of (et hanol) loaded IBMX was 2wt% of the mass of dry gel.

It can be stated, according to the results from paper I, that the prepared PNIPAM -copolymer gels exhibited higher IBMX binding capacity than PNIPAM gel at 35°C. The release rates of IBMX from the gels slowed down by the aromatic moieties in the polymer network, especially above LCST. The binding of IBMX to the polymers is concluded to be due to both the specific complex formation between aromatic moieties and IBMX, and to hydrophobic interactions inside the hydrophobically modified PNIPAM.

3.2 MICROGEL PARTICLES

3.2.1 PHASE TRANSITION AND COLLOIDAL PROPERTIES OF PARTICLES IN H_2O (II – IV)

It is well known, that at temperatures above the cloud point, linear PNIPAM in aqueous solution tends to precipitate, and eventually sediments from the solution as the system becomes unstable. The precipitation process can be followed by measuring the turbidity (optical transparency) of the solution with changing temperature or with time at constant temperature. The occurrence of precipitation and sedimentation is, as is typical to a phase-transition behaviour in a binary system, is dependent on the polymer concentration in the solution. However, colloidal stability of the formed PNIPAM –globules above the LCST can be adjusted by controlling both the concentration and the structure.[10]

The PNIPAM –based microgels prepared in this work (with SDS and MBA), show colloidal stability above the LCST, as expected from numerous earlier studies.[2, 21] In colloidal aqueous microgel systems, the particle concentration may be low, but the PNIPAM concentration inside the particles is high. Similarly also the concentration conditions in the core of the microgel particles compared to the surface layer are assumed to differ significantly. During synthesis at elevated temperatures the aqueous microstructure is locked by crosslinking. Particle size, internal microstructure and surface nature are governed by the self-assembling of the PNIPAM globules in the synthesis conditions. These conditions can be influenced by changing the amount of SDS and MBA.

Turbidity of colloidal microgel particles

With PNIPAM microgel particles high turbidity (milky appearance) of aqueous dispersion below the cloud point temperature indicates the presence of a significant fraction of permanent, solid particle structures evolved during the precipitation crosslinking polymerisation. These aqueous systems containing microgel particles are not turning transparent below the LCST as the densely packed and crosslinked particle cores are not solubilising. Turbidity observed at temperatures below the cloud point of PNIPAM increases with increasing crosslinker concentration in as shown in figure 5 a. Evidently more solid particle structures are formed during syntheses with large amounts of MBA. To compare the changes of turbidity with temperature for different microgels, the normalised changes of optical densities with temperature are shown in figure 5 b. In this case the measured

absorbance values at 20°C were taken as points of zero and the absorbance values were divided with the highest absorbance to normalise the data. According to the turbidity from the microgels prepared in 6.7 mM SDS solution, the phase transition shifts towards higher temperatures and broadens with increasing crosslinker concentration. The normalised turbidity data from the microgel M1.6, prepared with the lower SDS concentration, is plotted in the figure for comparison. M1.6 shows fairly broad phase transition, although the MBA concentration used in its synthesis was low. Figure 5 c shows, that there is not any or there is neglible amount of solid (insoluble) structures at temperatures below the cloud point in the microgel samples produced in high SDS concentrations compared to the samples synthesised in lower SDS concentrations.

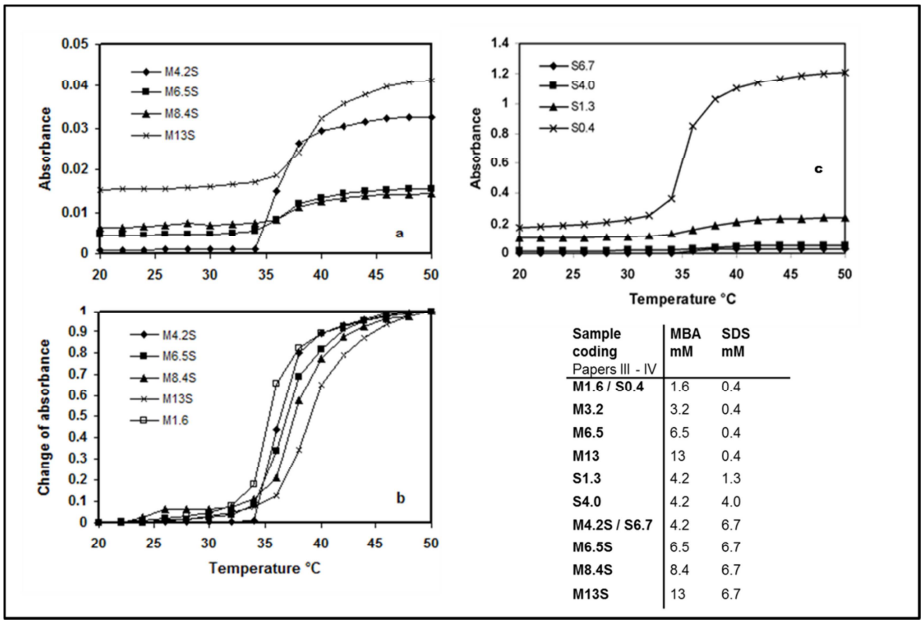

Sample coding Papers III - IV	MBA mM	SDS mM
M1.6 / S0.4	1.6	0.4
M3.2	3.2	0.4
M6.5	6.5	0.4
M13	13	0.4
S1.3	4.2	1.3
S4.0	4.2	4.0
M4.2S / S6.7	4.2	6.7
M6.5S	6.5	6.7
M8.4S	8.4	6.7
M13S	13	6.7

Figure 5. a) and c) The change of optical density (measured absorbance at λ 500nm, experimental errors < 0.005) with temperature for different microgels b) The normalised change of optical density with temperature for different microgels (1g/l in H_2O, heating rate 12℃/h from absorbance at wavelength 500 nm). The sample coding is given in the table embedded to the figure.

Particle sizes and zeta-potentials

The role of SDS in the particle nucleation is to increase the colloidal stability of precursor particles and thus lower the diameter of primary particles as the number of particles is increased. [21,71] The recipes reported by Wu et al. were applied in the preparation of the microgel samples. The highest SDS concentration reported in the case of Wu et al. was 4 mM, but usually the surfactant concentration in their study was 10 times lower. At SDS concentration range 0.2-4 mM, a dependence of the hydrodynamic diameter of the microgel (volume averaged by DLS at 50°C) from the SDS molarity has been found to follow the equation: log(diameter, nm) = -0.71*log(SDS molarity).[21,71] Corresponding microgels prepared in 0.2-4 mM SDS solutions have also been studied by McPhee et al. They found the average hydrodynamic diameter (intensity weighed from DLS at 25°C) becoming constant with the highest SDS concentrations, above 2 mM SDS.[71] Arleth et al. reported the use of 5.3 mM SDS concentration and a resulting small-sized (R_h ca. 50 nm at RT), structurally homogeneous (uniform radial crosslinker density) aqueous microgel structure, as indicated by the data from their SANS measurements below and above the phase transition temperature. Their data from SANS and DLS was consistent with a model of slightly polydisperse spherical particles.[27] In our case, one of the microgels, S6.7, was prepared in even higher SDS concentration, 6.7 mM. The intensity weighed size distributions at 20°C are shown in Figure 6 together with the sample coding and other analysis data in the table. As expected, the increase in the SDS concentration in the polymerisation batch decreases the hydrodynamic size of the microgel, but also the polydispersity of the product microgel appears to be increasing as can be concluded from the size distributions of samples S1.3, S4.0 and S6.7 prepared with equal amounts of crosslinker (Figure 6).

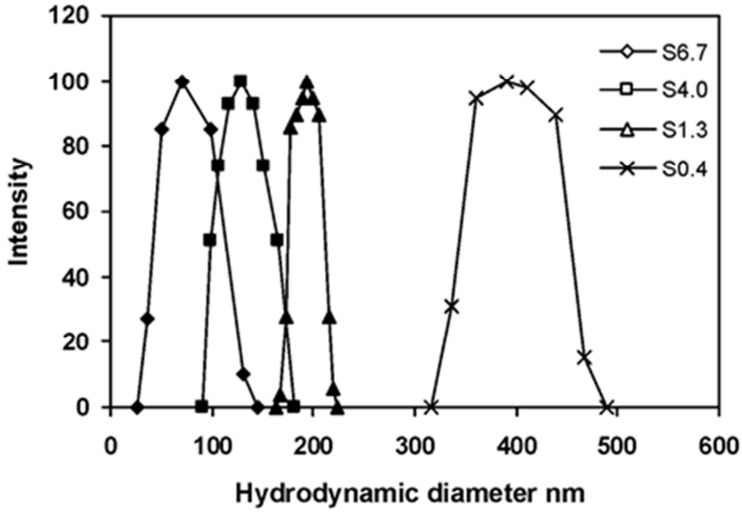

Sample coding Papers III - IV	MBA mM	SDS mM	[a]R_h 20°C nm	[a]R_h 50°C nm	[b]ζ 20°C mV	[b]ζ 40°C mV
M1.6 / S0.4	1.6	0.4	200	92	-2.4	-40.7
M3.2	3.2	0.4	196	101	-4.1	-41.2
M6.5	6.5	0.4	190	100	-15.0	-37.6
M13	13	0.4	202	126	-15.5	-40.2
S1.3	4.2	1.3	97	46	-16.9	-41.5
S4.0	4.2	4.0	65	29	+2.1	-3.1
M4.2S / S6.7	4.2	6.7	35	19	+2.1	-0.8
M6.5S	6.5	6.7	47	21	+1.8	-1.2
M8.4S	8.4	6.7	54	22	+1.4	-0.7
M13S	13	6.7	44	29	+1.1	-1.9

Figure 6. The intensity weighed size distributions of particles from DLS in aqueous dispersions at 20℃. Sample details and more inform ation is given in the embedded table.

The microgels are most likely stabilised against coagulation at elevated temperatures by electrostatic repulsion between the anionic surface groups originating from the polymerisation initiator fragments and the residual surfactant. This assumption is supported by the measured negative values of zeta potential (ζ) at 40°C for all the aqueous microgels listed in the table in Figure 6. In all cases the value of zeta potential becomes more negative as the temperature is increased above the LCST of PNIPAM. The zeta potentials are calculated from the values of the measured electrophoretic mobilities. The results discussed here are consistent with the earlier reports showing, that typically the electrophoretic mobility, and consequently the value of zeta potential, of PNIPAM microgel particles in aqueous dispersions (colloidally stabilised by negative charges) becomes more negative as temperature is

raised above the critical temperature.[87,71] With samples S1.3, S4.0 and S6.7 the zeta potential at 40°C is increasing with decreasing SDS concentration in the synthesis. The lowest values at 40°C, ca. -40 mV, were observed for the samples S0.4 and S1.3, prepared with the lowest amounts of SDS. Daly and Saunders have reported a zeta potential of ca. -38 mV measured with corresponding method (calculated with the Smoluchovski approximation) at 46°C for a PNIPAM microgel particle in pure water (R_h ca. 500 nm at 25°C). The particles were electrostatically stabilised by the negative charges from the polymerisation initiator fragments. In the particle preparation they used the surfactant-free method.[24]

The values of the zeta potential show a clear difference between the microgels prepared with the low and the high surfactant concentration. This is evident, when the zeta potentials of S1.3 (negative value) and S4 (positive value) are compared. Such complete change of surface nature indicates significant microstructural changes. According to the optical densities in Figure 5 c, the higher SDS concentration in the synthesis batch is concluded to prevent the formation of permanent, solid PNIPAM particles that would cause turbidity of the aqueous dispersions below the cloud point in the case of S4.0 compared to S1.3. It can be concluded, that at high SDS concentrations during the synthesis the precipitation of PNIPAM is decreased and consequently tightly packed PNIPAM particle cores are not formed. In other words more homogeneously structured PNIPAM microgels are resulting. Negatively charged species are not accumulated on the particle surfaces as in the cases of the particles with the solid cores to be stabilized. The figure below summarises the main particle features (optical transparency, hydrodynamic size, surface charge in aqueous dispersion) with changing SDS and MBA concentrations during synthesis. The illustration is drawn by taking into account the results of this study as well as the literature reviewed in chapter 1.2.2. The effect of MBA is not as dramatic as the effect of SDS, but still clear. Increasing hydrodynamic radius above the cloud point is observed with increasing MBA. This is reflecting the increasing size of the tightly crosslinked and rigid particle core. Tighly crosslinked particles show also more negative zeta potential compared to their lightly crosslinked comparisons. The results of this study are in good correlation with the thorough earlier literature on microgel-structures. On this safe basis, during the next chapters, it is aimed to rationalise the results of microcalorimetry and NMR –characterisation taking into account the structural heterogeneities. The structural indications of PNIPAM-microgels are not as thoroughly studied with these methods.

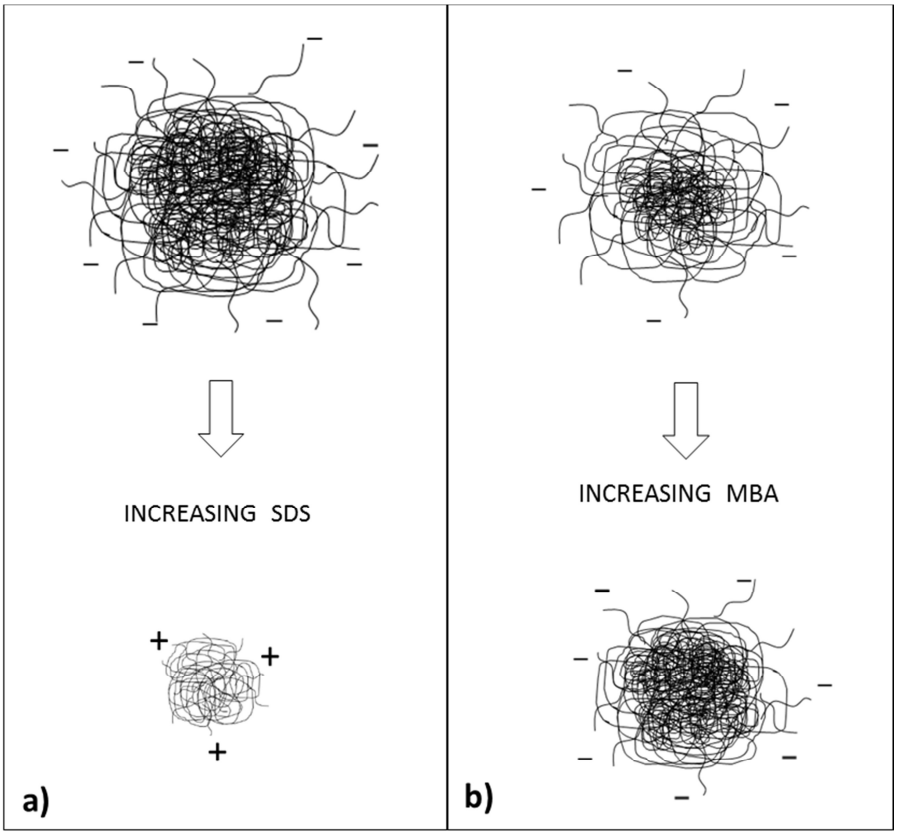

Figure 7. A representation of adjusting the particle features (optical transparency, hydrodynamic size, surface charge in aqueous dispersion) by changing the **a)** SDS and **b)** MBA concentrations during synthesis. The described homogeneous microgel is described on the left side with increasing SDS and compared to the other, more heterogeneous structures (as reflected by high turbidity).

3.2.2 THERMODYNAMIC PARAMETERS OF VOLUME PHASE TRANSITION IN H_2O (III, IV)

The calorimetrically obtained transition temperature of PNIPAM based polymers is often defined as the onset of the DSC transition endotherm, T_{onset} (the intersection of the baseline and the leading edge of the endotherm). The temperature of the maximum heat capacity, T_{max} , is also used to describe the transition temperature. For a sharp peak in a DSC thermogram it is possible to determine T_{onset} very precisely. However for broad peaks the determination of T_{onset} is more difficult due to inaccuracy in setting the baseline and in such cases it appears to be more reliable to determine the T_{max} in comparative studies.

The transition temperatures (T_{max}) versus MBA concentration in the synthesis are presented in figure 8 a. for the assumed homogenous microgels (SDS 6.7 mM) and heterogeneous microgels (SDS 0.4 mM). The T_{max} increases with increasing crosslinker concentration, and the effect appears to be more pronounced in the case of the microgels prepared with the high SDS concentration. Higher transition temperatures are observed for the microgels prepared in 6.7 mM surfactant solution. The measured endotherms of dehydration were fairly broad in all cases, indicating certain level of heterogeneity in all the microgels, but smaller values for the width of the transition at half-height ($\Delta T_{1/2}$) are observed for the microgels prepared at the high SDS concentration compared to the low SDS concentration as shown in figure 8 b. Clearly the width of the transition increases with the increasing crosslinker concentration in both cases of SDS concentration. The values of calorimetric enthalpy of transition, ΔH_{cal} (per moles of NIPAM units), are correspondingly plotted against MBA concentration in the synthesis in figure 8 c. ΔH_{cal} decreases significantly with MBA concentration with the microgels prepared in 0.4 mM SDS solution. With the higher SDS concentration the corresponding effect of crosslinker concentration is not so significant, but in any case clearly observable. Very low enthalpy of dehydration per NIPAM units, observed for the sample prepared in 0.4 mM SDS concentration with the highest amount of MBA, indicates the presence of significant fraction of non-hydrated PNIPAM in the microgel structure as already suggested also by the colloid turbidities. The results appear to be in correlation with the idea of homogenous and heterogenous microgel structure.

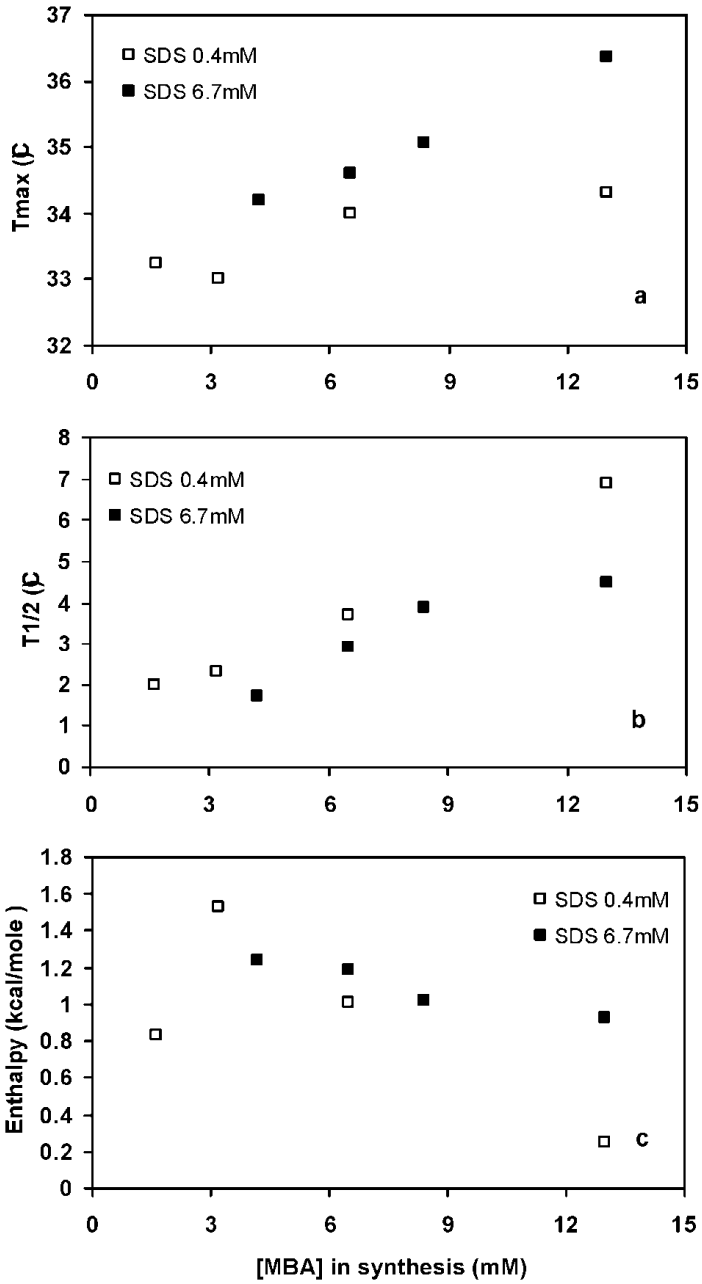

Figure 8. Thermodynamic parameters of volume phase transition measured with microcalorimetry from the aqueous microgels (1g/l, heating rate 30℃/h). a) The temperature of the maximum heat capacity (T_{max}, maximum errors +/- 0.3%) b) the width of the transition at half-height ($\Delta T_{1/2}$, maximum errors +/-0.3%) and c) the calorimetric enthalpy of transition, ΔH_{cal} (per moles of NIPAM units, maximum errors +/- 4%), versus MBA concentration in the synthesis batch.

From earlier studies of PNIPAM in aqueous surroundings it is known, that the heating rate and additive molecules (such as SDS) affect to microcalorimetric endotherms of dehydration. The effect of added SDS to the dehydration of PNIPAM microgel-particles have been studied microcalorimetrically by others. At heating rate 60°C/h and with PNIPAM microgel concentration 0.48% in water, the measured values of T_{max} were 35.0°C, 35.8 °C and 45.6°C in SDS concentrations 0 mM, 2 mM and 6 mM, respectively.[88] Taking into account the effect of added SDS, it appears, that the purified microgels in our case do not contain very large amounts of residual SDS from the synthesis batch. In our study, the microcalorimetric thermograms were recorded also by using the higher heating rate, 60°C/h. 0.1-0.5°C higher values of T_{max} and slightly broader endotherms of dehydration were obtained with the higher heating rate (data not shown here, see Paper III). Ding and coworkers reported similar effects of heating rate to the microcalorimetric data of linear PNIPAM (M_w $1.6*10^6$ g/mol) in water.[89] Similar HS DSC results as function of heating rate has been obtained also for 10µm-sized PNIPAM gel (MBA as crosslinker) particles suspended in water. [90] The gels were prepared in the good-solvent conditions and their structure can be assumed to be more homogeneous compared to microgels prepared in the poor-solvent conditions. Both samples, the linear PNIPAM[89] and the PNIPAM hydrogel[90], gave considerably more narrow endotherms of dehydration than were measured for PNIPAM microgels with various crosslinker (MBA) densities by Woodward and coworkers.[28] Woodward and coworkers investigated the volume phase transition of colloidal PNIPAM microgels prepared with varying crosslinker concentrations (0.25-30 % of MBA in monomer mixture) by surfactant-free emulsion polymerisation. DSC analyses of these aqueous microgel particles showed that the T_{max} and the width of the volume phase transition increase with increasing crosslinker concentration. For example, T_{max} of the calorimetric endotherm increased by about 2°C when the amount of MBA in the monomer mixture was increased from 0.5% to 5%. The calorimetric enthalpy change of the transition decreased with increasing crosslinker concentration. In their study, the calorimetric results were explained as being due to a relatively more rigid structure of the microgel at higher crosslinker concentrations, a result of increasing rigidity the volume phase transition broadens and it is pushed towards higher temperatures. Similar trends with MBA concentration were observed in our case, even when SDS is used as a surfactant during synthesis.

3.2.3 VOLUME PHASE TRANSITION OBSERVED FROM THE NMR SIGNAL INTENSITIES IN D_2O (II-IV)

The phase transition in microgels was studied more closely on molecular level by quantitative ^1H NMR spectroscopy in D_2O. By NMR in liquid state we can monitor the mobile, soluble, structures and possible solid structures in samples cannot be analysed. It has to be noted, that H_2O was used as a solvent in the microcalorimetric measurements. When comparing the NMR results to the calorimetric results it is useful to keep in mind that H_2O and D_2O differ in their physical properties and that a hydrogen bond in D_2O is ca. 5% stronger.[91] PNIPAM coils are suggested to be more extented in D_2O below the critical temperature and there may be a higher level of ordering of D_2O associated with a polymer chain.[92] Kujawa and Winnik[93] reported for linear PNIPAM (of molecular weight ca. 300000 g/mol) a very similar microcalorimetric endotherm in general features in D_2O compared to the corresponding endotherm in H_2O. But in comparison to H_2O, an increase of T_{max} by 0.6°C and a doubling of the change of heat capacity occurring upon the phase transition was observed in D_2O. Also it has to be noted that the parameters of transition by microcalorimetry were obtained at heating rates 30 and 60°C/h, whereas the NMR-data was collected after stabilising the sample after heating steps (2-5°C/step) for 30 minutes.

During the volume phase transition the signal intensities of the main chain methylene (ca. 1.5 ppm) and methyne (ca. 2 ppm) protons decrease considerably already at 25-30°C and the signals disappear completely at 50°C. Instead, the methyl protons (ca. 1 ppm) and the lone proton (ca. 4 ppm) of the N-isopropyl group show corresponding rapid response at temperatures closer to the cloud point of PNIPAM at 32-35°C and the side chain proton signals can be detected even above 50°C as small ones. At temperatures above 35°C we are most likely observing proton signals only from the surface of the collapsed particle, since only soluble and mobile can be analysed with this method. Corresponding observations have been reported for linear PNIPAM.[62,69] The spectral changes upon heating can be used to compare the microgel structures.

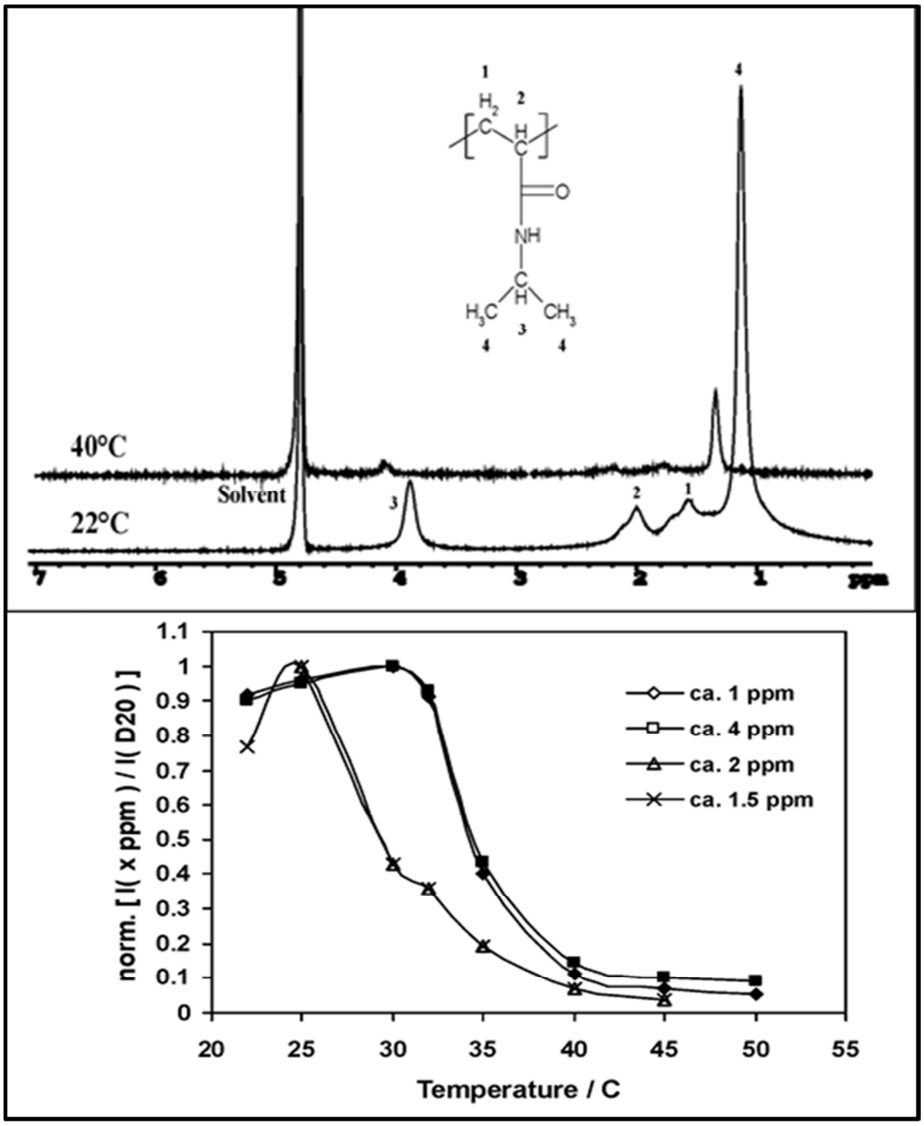

Figure 9. In the upper figure, a typical ^{1}H NMR spectra recorded at 22℃ and at 40℃ in D_2O for microgels (N1 and N2, Paper II). In the lower figure, normalised ratios of ^{1}H NMR signal intensity (I) of the PNIPAM protons to the solvent (D_2O) protons versus temperature as measured for the protons of the N-isopropyl group (methyl protons ca. 1 ppm and the lone proton ca. 4 ppm) and the protons of the main chain (methylene protons ca. 1.5 ppm and methyne protons ca. 2 ppm).

The intensity data from the side chain protons in Figure 10 a suggests that the phase transition is not significantly affected by the MBA concentration. However, the same data analysed for the methyne protons in the main chain (2 ppm) in Figure 10 b suggests otherwise. The increasing MBA concentration decreases significantly the response temperature of the main chain protons of sample M6.5, and the decrease of intensity of the proton signals occurs at broader temperature range. According to the Figure 10 c, increasing SDS concentration increases the transition temperature, as already suggested by the results of microcalorimetry in Figure 8.

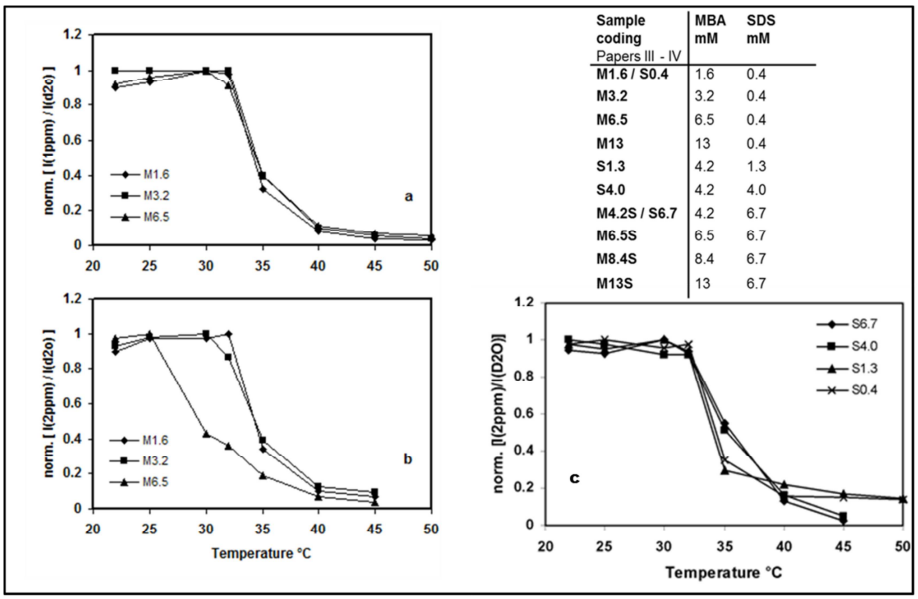

Sample coding Papers III - IV	MBA mM	SDS mM
M1.6 / S0.4	1.6	0.4
M3.2	3.2	0.4
M6.5	6.5	0.4
M13	13	0.4
S1.3	4.2	1.3
S4.0	4.2	4.0
M4.2S / S6.7	4.2	6.7
M6.5S	6.5	6.7
M8.4S	8.4	6.7
M13S	13	6.7

Figure 10. Normalised ratios of the ^{1}H NMR signal intensity (I) of the a) methyl protons (side chain, ca. 1 ppm), b) and c) methyne protons (main chain, ca. 2 ppm) to the solvent (D_2O, ca. 4.8 ppm) protons versus temperature in different samples (coding given in the embedded table).

3.2.4 DYNAMIC BEHAVIOUR OF POLYMER SEGMENTS FROM THE NMR RELAXATION TIMES (II- IV)

Dynamic behaviour of PNIPAM chains in the microgels was studied by measuring spin-lattice (T_1) and spin-spin (T_2) relaxation times of the side chain and the main chain protons at temperatures 22-50°C in D_2O (Figures 11-13). The relaxation decays were monoexponential, indicating that the signal is coming from the most mobile and most abundant species in the systems. This means that signal from the significantly less mobile parts of the polymers is not reflected in the relaxation data due to a very quick relaxation. When analysing the structural connections of the relaxation times, the broad temperature range of study is divided in two parts. See the table 5 for the guidelines.

Table 6. *Guidelines for correlating the relaxation times of PNIPAM-microgels in D_2O.*

At temperatures below the LCST	**At temperatures above the LCST**
High proton signal intensities	Low proton signal intensities
Good accuracy of exponential analysis of the relaxation times	Errors of exponential analysis increase
Interpretation Swollen network dominates the signal	Interpretation Charged, coronal surface layer is still mobile after the network has collapsed (high local LCST)

In general the increase of T_1 with temperature, as the spin –lattice relaxation slows down, is concluded to be due to decreasing mobility during the phase transition. Similarly the spin-spin relaxation times (T_2) higher values are concluded to indicate structures with higher mobility. At first sight the trends of the relaxation times with changing temperature appear to be too complicated for any conclusions (Figures 11-13). However, if the suggested significant structural changes with crosslinker concentration, and especially with SDS concentration are taken into account, the results can be rationalised. In the assumed homogeneous microgel structure also charges are more evenly distributed compared to the corresponding heterogenous microgel structure with highly charged surface and insoluble core. As the zeta potentials were suggesting, the negatively charged coronal layers (with high local LCST) in the heterogeneous microgels are likely to contribute to the proton signals well above the LCST.

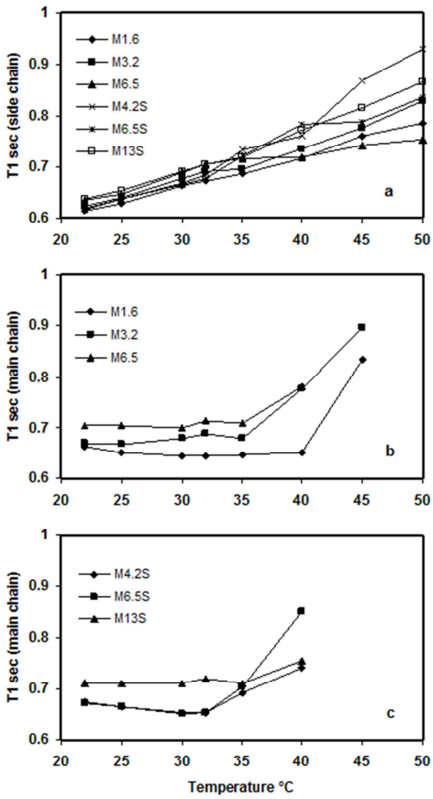

Fig. 11

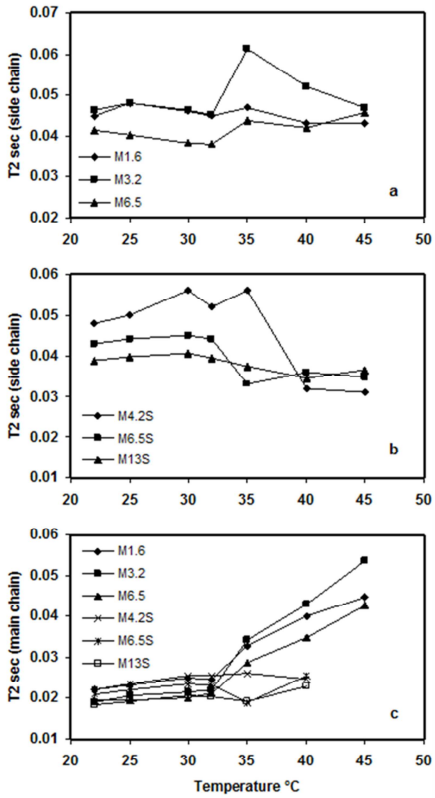

Fig. 12

Figure 11. ^{1}H NMR relaxation times measured from the microgels in D_2O. a) Spin-lattice relaxation times (T_1) of the methyl protons (side chain, ca. 1 ppm). Spin-lattice relaxation times (T_1) of the methyne protons (main chain, ca. 2 ppm) for the microgels prepared b) in 0.4 mM and c) in 6.7 mM SDS solution.

Figure 12. ^{1}H NMR relaxation times measured from the microgels in D_2O. Spin-spin relaxation times (T_2) of the methyl protons (side chain, ca. 1 ppm) for the microgels prepared a) in 0.4 mM and b) in 6.7 mM SDS solution. c) Spin-spin relaxation times (T_2) of the methyne protons (main chain, ca. 2 ppm)

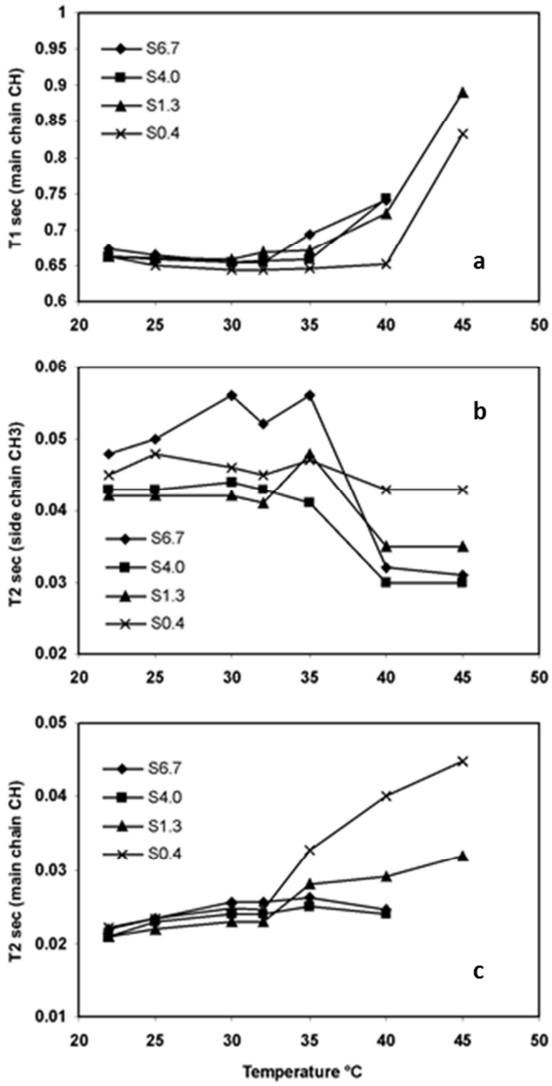

Figure 13. a) Spin-lattice relaxation times (T_1) of the methyne protons (main chain, ca. 2 ppm), b) spin-spin relaxation times (T_2) of the methyl protons (side chain, ca. 1 ppm) and c) spin-spin relaxation times (T_2) of the methyne protons (main chain, ca. 2 ppm) versus temperature for different samples in D_2O

The T_2-curves vs. temperature for side chain (methyl) show a step towards lower values at transition temperature (see Figures 12 b and 13 b). The magnitude of the step is increasing with decreasing MBA (in high SDS series, Figure 12 b). The result corresponds to the general idea of increasing swelling

ratio with decreasing MBA and increasing molecular mobility. Such clear behaviour of T_2 is not observed with samples prepared by low SDS (Figure 12 a). This is concluded to be due to the heterogenous structure complicating the analysis. The magnitude of the T_2- step is also increasing with increasing SDS (Figure 13 b). As already concluded from turbidities, high SDS decreases the precipitation crosslinking during synthesis, and this is likely to produce more homogenous and soluble microgel structure. The T_2-curves vs. temperature for main chain (methyne) are very different for the microgels synthesised with low and high SDS concentrations (Figures 12 c and 13 c) reflecting again the structural difference. Above the transition T_2-values for high SDS samples (M4.2S-M13S, S4.0, S6.7) could not be analysed due to too low signal intensities. However the T_2-curves show a clear upward trend above 32°C, by the structures still very much soluble. These signals could also be originating from the charged surface layer with high local LCST (Figures 12 c and 13 c).

Table 7. *Summary of the structural conclusions from the relaxation times*

T_1 side chain	**T_2 side chain**
-trends are similar for all samples -differences increase above the LCST -this relaxation is not especially sensitive to particle structure **See Figure 11 a.**	-large decrease of T_2 at LCST (the gel collapse shows clearly for a homogeneous gel) -for a heterogeneous gel such stepwise change not to be seen **See figures 12 a , 12 b and 13 b.**
T_1 main chain	**T_2 main chain**
-signals still visible for coronal layers at 45°C -for homogenous structures signals disappear **See figures 11 b, 11 c and 13 a.**	-for heterogeneous structures increase in T_2 by coronal layers at high temperatures -for homogenous structures signals disappear **See figures 12 c and 13 c.**

Before this study there were only few reports of applying the liquid state NMR in the studies of the physical structure of PNIPAM microgels. Solvent diffusion measurements at various temperatures by the PGSE (pulsed-gradient spin-echo)-NMR had been reported, and later the same approach was used to study the effect of the crosslink density on the volume phase transition of PNIPAM microgels [28,58] The use of NMR methods for studying of PNIPAM systems with various aims in aqueous media was reviewed 2009

by Spevacek.[70] Generally it was stated, that NMR methods provide several promising tools for the research of the structure and interactions of PNIPAM in nano- and microstructures. However, it is clear that, the full potential of NMR methods with PNIPAM structures is not yet utilised. As methods sensitive to dynamic properties in the phase transition on molecular level, microcalorimetry and NMR spectroscopy support each other [33,43,94] and give a good addition to the scattering methods generally used for the structural studies of PNIPAM microstructures.

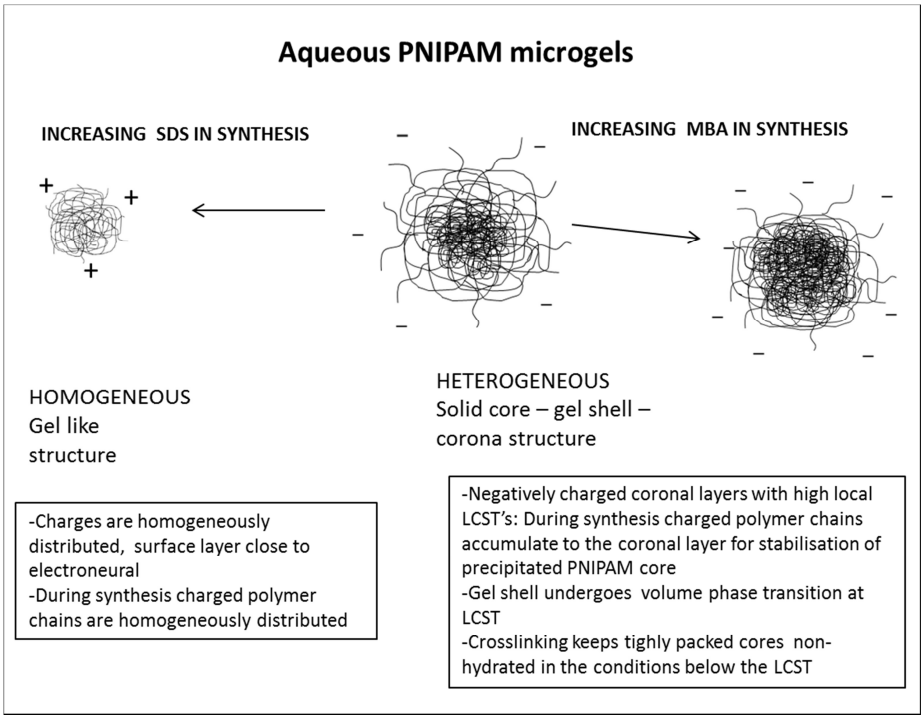

Figure 14. Summarising the structural variations in aqueous PNIPAM microgels.

3.3 MICROGEL PARTICLES WITH PS CORE (II)

As in the PNIPAM-microgel case, research publications of PNIPAM microgels on PS core using microcalorimetry or NMR are still scarcely available. Ballauff and coworkers studied the phase transition of PNIPAM-microgel as a shell on a polystyrene based core with numerous other methods as reviewed in 2007.[5,26,34-37] They prepared the core particles by conventional emulsion polymerisation of styrene and NIPAM (95/5 wt%) and as a second step they copolymerised NIPAM with the crosslinking monomer, MBA, in the presence of the core particles. Phase behaviour of the thermosensitive shell in aqueous particle dispersions was studied by combining the data from different scattering methods. Typically the core particles in aqueous dispersion were of approximately 100 nm in diameter and the crosslinked PNIPAM shell was of 10-50 nm in thickness depending on the temperature. It was shown that the PNIPAM shell in swollen state exhibited static and dynamic inhomogeneities, but clear evidences of radial distribution of crosslinks or inhomogeneities in the network were not found.

3.3.1 PHASE TRANSITION AND COLLOIDAL PROPERTIES OF PARTICLES IN H_2O

In our study 100% PS-particles of approximately 50 nm in diameter were used as seeds for the precipitation polymerisation of NIPAM in the presence of MBA. As expected from the earlier studies, the particle sizes grew during the second stage polymerisations. The largest 2-stage particle, PS2N, was synthesised by using a larger monomer to seed particle mass ratio compared to the syntheses of PS1N and PS1NA (synthesis summary in Table 3). The 2-stage particles show monomodal size distributions that are broader than the size distributions obtained for their seed particles. (Figure 15, upper) The mean hydrodynamic diameters of the 2-stage particles versus temperature at range 15°C-50°C are presented also in Figure 15 (lower). The mean hydrodynamic radius versus temperature for PNIPAM microgel particle, N1, is plotted in the figure for comparison. The microgel particle deswells rapidly within a temperature range 25-35°C and its radius decreases nearly 50% upon heating at the studied temperature range. The 2-stage particles deswell gradually through the whole studied temperature range showing nearly linear deswelling. As an exception a clear deviation from linearity is observed for PS2N at temperature range 30-40°C. Behaviour of PS2N differs from the other particles since its total volume decrease upon heating is very small compared to its original size at 20°C. The size distributions in all cases

remained monomodal and particle coagulation was not observed during the measurements. The particles are most likely stabilised against coagulation at elevated temperatures by electrostatic repulsion between the anionic surface groups originating from the polymerisation initiator fragments, residual surfactant and in addition from the dissociated carboxylic acid groups in the case of PS1NA.

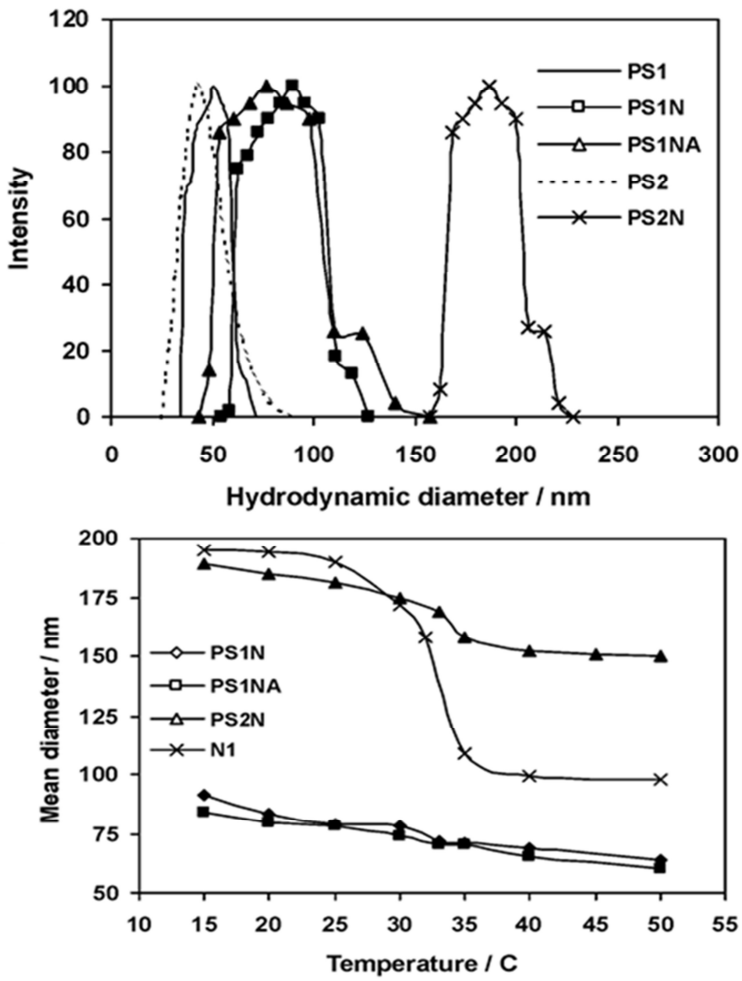

Figure 15. Upper figure: The intensity weighed size distributions of particles in aqueous dispersions at 20℃. Lower figure: The mean hydrody namic diameters of the 2-stage particles versus temperature. The the microgel particle, N1, is plotted in the figure for comparison. Sample coding for microgel particles

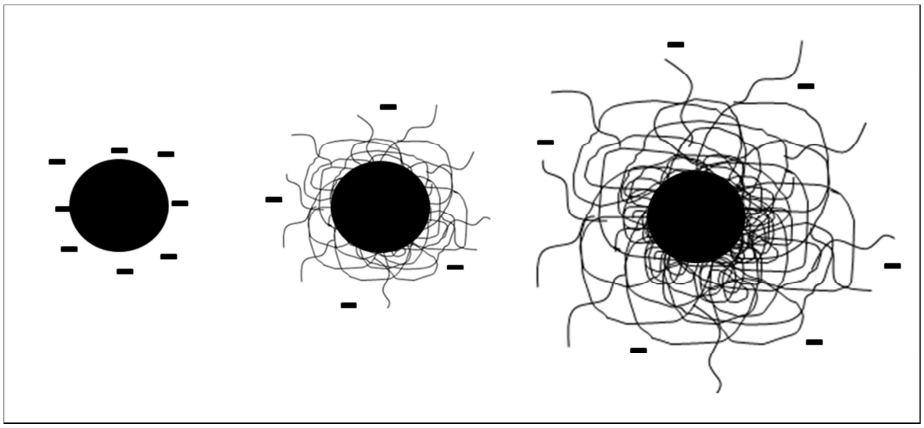

Figure 16. A representation of a solid PS1/PS2-core particle (left), PS1N –core-shell (middle) and PS2N-core-shell (right)

In the studies by Ballauff and coworkers,[5,26,34-37] the volume phase transition of the shell was found to be continuous and the degree of shrinking was found to be much less than what is observed for macroscopic networks of a similar degree of crosslinking. This was suggested to be due to the fact that macroscopic networks shrink along three directions whereas the shell networks on a rigid core can only shrink in the dimension along the surface normal. Our DLS results on volume phase transition of PNIPAM microgel on solid PS core are supporting their results.

3.3.2 THERMODYNAMIC PARAMETERS OF VOLUME PHASE TRANSITION IN H_2O

The endotherms are presented here as excess heat capacities versus temperature. See Figure 17 below for details. Broader endotherms are observed for crosslinked PNIPAM in the 2-stage particles compared to the reference microgel sample, N1. Especially in the case of PS2N a clear increase of T_{max} can be observed. It is to be concluded, that the phase transition of crosslinked PNIPAM in the shell has shifted towards higher temperatures when compared to the microgels and also that the temperature range of the transition is broader. The thermodynamic parameters for the 2-stage particle PS1NA are listed in the table below, showing a very broad endotherm of dehydration. The presence of acrylic acid, as a hydrophilic comonomer in the microgel –shell is logically the source of the observed endotherm broadening. Acrylic acid (AA) as the hydrophilic comonomer creates areas of high local LCST to the shell layer giving rise to increased structural heterogeneity. However, more samples of solid core – PNIPAM microgel shell structures with different chemistries should be studied with microcalorimetry to discuss this in more detail.

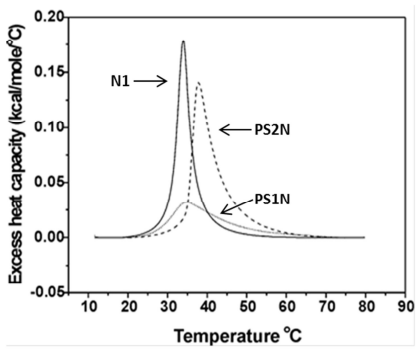

Sample 30°C/h	N1 2 g/l	PS1N 20 g/l	PS2N 2 g/l	PS1NA 20 g/l
T_{max} °C	34.0	34.8	37.8	36.6
$T_{½}$ °C	3.7	13.5	6.1	24.1
ΔH_{cal} kcal/mole	1.01	0.52	1.21	0.53

Figure 17. Microcalorimetric endotherms (heating rate 30℃/h) f or aqueous dispersions of the microgel and the 2-stage particles.

Zhu and Napper pioneered the experimental studies on coil-to-globule transitions of linear PNIPAM chains attached to the surfaces of polystyrene latex particles.[30,31] Studies showed broadening of transitions of interfacial chains compared to free chains in solution. The broad overall transition of the interfacial chains was explained to consist of two components. Upon heating first the inner region of each chain adopts its globular form whereas the segments of chains in coronal layer exist in the coil-like conformation until the LCST is reached. There are interesting results reported also for PNIPAM on other solid particle surfaces. The phase transition of low molecular weight PNIPAM (ca. 5000 g/mol) covalently bound to the surface of gold clusters of few nm in size have been investigated with microcalorimetry by Shan and coworkers. [32] The PNIPAM chains as monolayer exhibited two separate transition endotherms of dehydration around the LCST. The first transition with a sharp and narrow endothermic peak was observed at lower temperature while the second one with broader peak was observed at higher temperature. As in the case of Zhu and Napper[30,31] it was suggested, that the inner segments of chains close to the particle surface are densely packed and less hydrated showing the first transition while the segments in coronal layer are more hydrated showing the second transition. As methods sensitive to dynamic properties in the phase transition on molecular level, both microcalorimetry and NMR spectroscopy have been employed to investigate the high molecular weight (3.5 *105 g/mol) PNIPAM adsorbed on silica particles. [33] In that case, again, the effect of the solid surface was an increased transition temperature and a broadening of the transition. Both effects were more pronounced at low surface coverage. The studies of phase transition showed that PNIPAM chains on solid particles exhibits very different and more complex dynamic properties compared to volume systems in microgels.

3.3.3 VOLUME PHASE TRANSITION OBSERVED FROM THE NMR SIGNAL INTENSITIES

The 2-stage particle PS1N shows more gradual decrease of methyl proton signal through the whole studied temperature range (Figure 18). Poly(NIPAM-co-acrylic acid) microgel structure in the 2-stage particle PS1NA appears to be quite swollen in D_2O even at 50°C due to the presence of the hydrophilic comomonomer units. According to the results from the signal intensities with temperature PS1N shows a broader transition than PS2N. Observations from the NMR signal intensities are in good agreement with microcalorimetry.

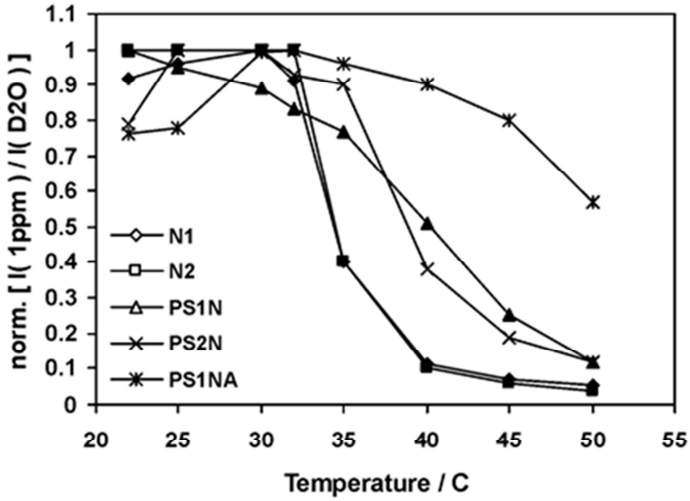

Figure 18. Normalised ratios of the ^{1}H NMR signal intensity (I) of the methyl protons (ca. 1 ppm) to the solvent (D_2O) protons versus temperature in different particles.

3.3.4 DYNAMIC BEHAVIOUR OF POLYMER SEGMENTS FROM THE NMR RELAXATION TIMES

Figure 19 a shows the temperature dependence of the T_1 for protons of the side chain methyl groups in the studied particles. For all samples T_1 increases with temperature showing close to linear dependence. It appears that T_1 of the side chain methyl protons is not highly sensitive to the particle structure, since the T_1 values measured for different particles at the same temperature deviate from each other only with some tens of milliseconds. The result is in correlation with observations for the microgels in chapter 3.2.4.

Larger differences between the particles are observed when looking at the corresponding T_1 data for the main chain methyne protons in figure 19 b. In general the 2-stage particles show lower values of T_1 for main chain methyne protons than the reference microgels and the sample N1 shows again the highest T_1 values. This may be an indication of more mobile structures of PNIPAM in the 2-stage particles than in the microgel samples. Above 35°C it appears, that the signals are analysable for the 2-stage particles at higher temperatures than for microgels. The broadening of their volume phase transition towards the higher temperatures was already shown by microcalorimetry.

Figure 19 c shows the temperature dependence of the T_2 for protons of the main chain methyne groups in the studied particles. At temperatures below 35°C the 2-stage particles show clearly higher T_2 values than the microgel particles. Higher T_2 values refer again to more mobile components existing in 2-stage particle samples and possible explanation is a looser and / or more heterogeneous network structure of PNIPAM compared to the microgel samples. But as already stated in the microcalorimetry chapter, more similar core-shell samples should be analysed to discuss the relaxation time – structure correlations in more detail.

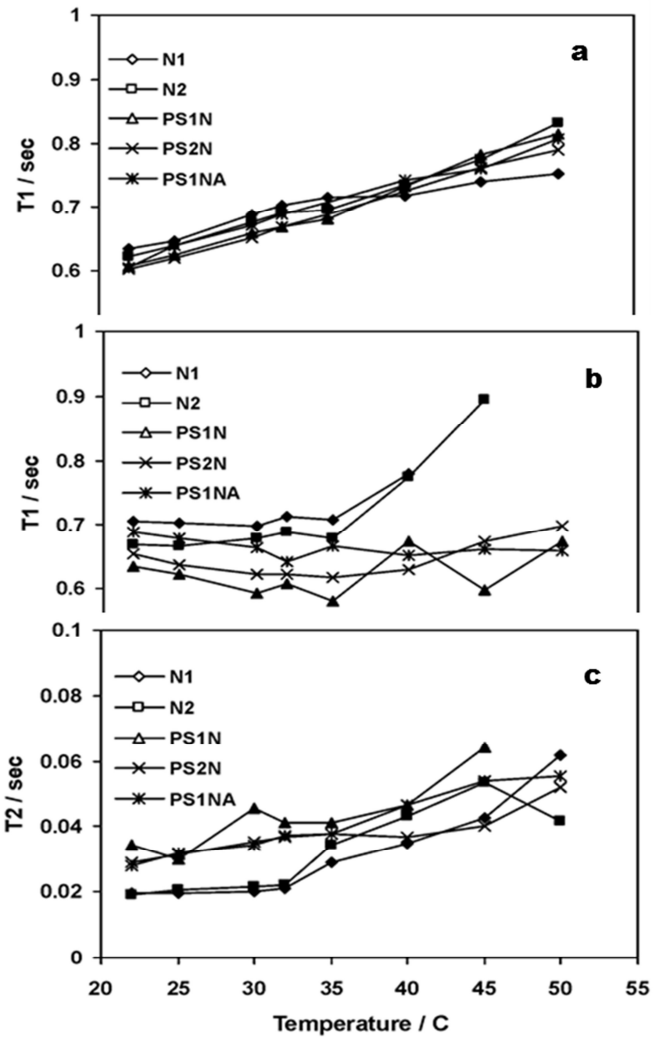

Figure 19. a) Spin-lattice relaxation times (T_1) of the methyl protons (side chain), b) Spin-lattice relaxation times (T_1) of the methyne protons (main chain) , c) Spin-spin relaxation times (T_2) of the methyne protons (main chain) versus temperature for different particles in D_2O

3.4 FLUORESCENT PARTICLES IN APPLICATION STUDIES

3.4.1 CELL–POLYMER INTERACTIONS OF MICROGEL PARTICLES WITH PS CORE (V)

As a part of Academic Dissertation by H. Vihola in 2007[95] the results of paper V have been earlierly reviewed. Fluorescent PS-particles with different surface coatings were prepared for the cell-polymer interaction studies with a collaborating research group in pharmaceutical technology. The detailed synthesis information for particle samples coded as FPS, FPS-PNIPAM and FPS-PEO and used in the study are reported in the original paper and are briefly described here in chapter 2 (Table 4). PNIPAM microgel particles with PS core (FPS-PNIPAM) were prepared similarly to the syntheses of PSN-coded particle series described in Paper II, but with the exception of using the fluorescent polystyrene (FPS) particles as seeds in the crosslinking polymerisation of NIPAM.

In Paper V, the cell–polymer interactions of PS particles with different surface chemistries (crosslinked PNIPAM and PVCL, PEO-grafts) were studied. In this study the effects of temperature and the nature of the polymer coating on the cellular interactions were evaluated by cell association/uptake and visualized by confocal scanning microscope. It was concluded, that PNIPAM coating inhibited the polymer–cell contact by steric repulsion similarly to PEO-grafts, whereas PVCL coated FPS was adsorbed on the cells more strongly, especially at 37 ^{0}C. This result with a PNIPAM shell is in correlation with the observed high T_2 (chapter 3.3.4.) values referring to mobile components existing in 2-stage particle samples still above LCST and supports the idea of local high LCSTs of coronal PNIPAM layers in the outermost parts.

4 CONCLUSIONS

In the first stage of the present research, the interest focused in developing a temperature controlled release system for a model drug, IBMX, based on a PNIPAM-microgel system with adjusted properties. Assuming that, if the drug binding and release properties of the polymer matrix within colloidal microgel particles can be influenced and controlled, it may be possible to obtain desired drug level in the applications, where it is not possible to administere the drug by injections. By altering temperature and ionic strength, it should be possible to bind and release IBMX controllably. It is concluded, according to the results from paper I, that the prepared macroscopic PNIPAM -copolymer gels, with properties adjusted chemically by adding the aromatic esters groups (benzoates and cinnamates) to the structures, exhibited higher IBMX binding capacity than the unmodified PNIPAM gel in pure water. The release rates of IBMX from the gels are slowed down by the aromatic moieties in the polymer network, especially above LCST. The binding of IBMX to the polymers is concluded to be due to both the specific complex formation between aromatic moieties and IBMX, and to hydrophobic interactions inside the hydrophobically modified PNIPAM. After the publication of paper I, corresponding colloidal and chemically modified microgels were prepared and preliminarily tested for the application in physiological salt solution. This experimental data was not published, but it was observed that IBMX released from the microgels instantly and uncontrollably. The question arose, if the drug binding and release properties of macroscopic gels and those of colloidally stable microgels with corresponding chemical composition can be correlated at all because of the obvious structural differences.

After the paper I, the interest of the research was refocused to more detailed investigations of PNIPAM microgel structures in colloidal particles. There were on-going discussions and research papers published on the heterogeneous structures of PNIPAM microgels, but there were only few reports of applying the liquid state NMR in the studies. More structural knowledge on PNIPAM microgels was needed. In general, there was also a need for more information on the temperature dependence of the ^{1}H NMR spectra and the ^{1}H NMR relaxations of PNIPAM microgels. In the next part of the research, published in papers II-IV, the structural characteristics of microgels were studied with other methods in addition to NMR spectroscopy to compare the results above and below the LCST. The aim was to study the structures of PNIPAM microgels synthesised with different concentrations of surfactant (SDS) and crosslinking monomer (MBA), as well as PNIPAM-microgel as a shell on PS particle core.

Basic characterisation of colloidal microgel particles (optical densities, particle sizes and zeta potentials) was needed in order to rationalise the results from microcalorimetry and NMR spectroscopy. It was observed, that microgels are stabilised against coagulation at elevated temperatures by electrostatic repulsion between the ionic surface groups. The values of the zeta potential show a clear difference between the microgels prepared with the low (clearly negative value) and the high surfactant concentration (slightly positive value). The complete change of surface nature as the mode of particle stabilisation is altered, indicates also significant microstructural changes. According to the optical densities, the higher SDS concentration in the synthesis batch is concluded to prevent the formation of permanent, solid PNIPAM particles that would cause turbidity of the aqueous dispersions below the cloud point. With high SDS concentrations during synthesis, the precipitation of PNIPAM is prevented, and consequently tightly packed PNIPAM particle cores are not formed. In other words more homogeneously structured PNIPAM microgels are resulting. The concentration of MBA does not affect to the structure as dramatically as SDS, but the effect is clearly observed. Increasing hydrodynamic radius above the cloud point is observed with the increasing MBA concentration. This owes to the increasing size of the tightly crosslinked and rigid particle core. The tightly crosslinked particles show also more negative zeta potential compared to the lightly crosslinked ones. The results of this study are in good correlation with the earlier literature on colloidal properties of PNIPAM microgels.

Relying on this study and on few earlier reports on heterogeneous PNIPAM microgels, it is concluded that due to a relatively more rigid structure of the microgel at higher crosslinker concentrations, the volume phase transition broadens, and it is pushed towards higher temperatures. The enthalpy of transition (per moles of NIPAM units) in concluded to decrease with increased crosslinking density. According to this study, similar conclusion of the effect of MBA concentration is made also for the homogeneous microgels prepared in high SDS concentration.

Phase transitions and structural characteristics of microgels were further studied with ^{1}H-NMR spectroscopy including the measurements of the signal intensities as well as the spin-lattice (T_1) and spin-spin (T_2) relaxation times for the protons of PNIPAM with changing temperature.When analysing the relaxation times, the broad temperature range of study is divided in two parts, to cases above and below the LCST. When the suggested significant structural changes with the MBA concentration, and especially with the SDS concentration are taken into account, the results can be rationalised. In the homogeneous microgel structure also the charges should be more evenly distributed compared to the corresponding heterogeneous microgel structure with highly charged surface and insoluble core. As the zeta potentials were also suggesting, the negatively charged coronal layers (with high local LCST)

in the heterogeneous microgels are likely to contribute to the proton signals well above the LCST. Before this study there were only few reports of applying the liquid state NMR in the studies of the physical structure of PNIPAM microgels. As methods sensitive to the phase transition on molecular level, microcalorimetry and NMR spectroscopy support each other and give a good addition to the scattering methods generally used for the structural studies of PNIPAM microstructures.

The aim of the study, reported in paper II, was to obtain new information on PNIPAM microgels as a shell on solid polystyrene core particles compared to heterogeneous (also core-shell-like) PNIPAM microgels by applying especially NMR spectroscopy and microcalorimetry. Earlier studies had shown that PS core has significant effect to the phase behaviour of PNIPAM microgel shell. It is assumed that on solid core microgel can only shrink in the dimension along the surface normal, not on all three directions. However, during this study it has been concluded, that also the heterogeneous PNIPAM microgels most likely contain a solid-like PNIPAM core. From this perspective, it would be more useful to compare the PNIPAM microgels as a shell on solid polystyrene core with the homogenous PNIPAM microgels. To summarise, our results (DLS, microcalorimetry) with the microgel shells on PS core appear to follow the general trends reported for linear PNIPAM or microgel on solid particle surfaces. It is concluded, that the phase transition of crosslinked PNIPAM in the shell has shifted towards higher temperatures when compared to the heterogeneous microgels and also that the temperature range of the transition is broader. According to the relaxation times from NMR-studies, it can be concluded that there is more mobile structures of PNIPAM on PS core particles compared to the heterogenous microgel samples (a looser and/or more heterogeneous network structure). Above 35°C it appears, that the signals are analysable for at higher temperatures than for the microgels. Results in paper V show that PNIPAM microgel shell on PS core inhibited the polymer–cell contact by steric repulsion similarly to PEO grafts, whereas PVCL coated PS was adsorbed on the cells more strongly, especially above the LCST. This result with a PNIPAM shell is in correlation with the observed high T_2 values referring to mobile components existing in 2-stage particle samples still above LCST and supports the idea of local high LCSTs of coronal PNIPAM layers in the outermost parts. But to make more conclusions, similar core-shell samples should be studied further, to discuss the relaxation time – structure correlations in detail.

REFERENCES

1. Heskins, M.; Guillet, J. E. Macromol Sci Chem 1968, A2, 1441-1455
2. Schild, H. G. Prog. Polym. Sci. 1992, 17, 163-249
3. Winnik, F.M. Macromolecules 1990, 23, 233-242
4. Pelton, R. J. Coll. Int. Sci. 2010, 348, 673-674
5. Ballauf, M.; Lu, Y. Polymer 2007, 48, 1815-1823
6. Okano, T. (ed.), 1998, Biorelated polymers and gels, Academic Press, San Diego, USA, 29-68
7. Zhang, L.; Daniels, E. S.; Dimonie, V. L.;Klein, A. J. Appl. Polym. Sci. 2010, 118, 2502–2511
8. Nykänen, A.; Rahikkala, A.; Hirvonen, S.-P.; Aseyev, V.; Tenhu, H.; Mezzenga, R.; Raula, J.; Kauppinen, E.; Ruokolainen, J. Macromolecules 2012, 45, 20, 8401-8411
9. McKee, J. R.; Ladmiral, V.; Niskanen, J.; Tenhu, H.; Armes, S. P. Macromolecules 2011, 44, 19, 7692-7703
10. Aseyev, V.O.; Tenhu, H.; Winnik, F.M. Adv Polym Sci 2006, 196, 1-85
11. Adelsberger, J.; Kulkarni, A.; Jain, A.; Wang, W.; Bivigou-Koumba, A. M.; Busch, P.; Pipich, V.; Holderer, O.; Hellweg, T.; Laschewsky, A.; Müller-Buschbaum, P.; Papadakis, C.M. Macromolecules 2010, 43, 5, 2490-2501
12. Hoare, T.; Pelton, R. Langmuir 2008, 24, 1005-1012
13. Pelton, R.; Hoare, T. Microgels and Their Synthesis: An Introduction, in Microgel Suspensions: Fundamentals and Applications 2011 (eds A. Fernandez-Nieves, H. M. Wyss, J. Mattsson and D. A. Weitz), Wiley-VCH Verlag GmbH & Co. KGaA, Weinheim, Germany. doi: 10.1002/9783527632992.ch1
14. Nayak, S.; Bhattacharjee, S.; Chaudhary, Y.S. J. Phys. Chem. C 2012, 116, 1, 30–36
15. Tanaka, T., Phys. Rev. Lett. 1978, 40, 820-823
16. Tanaka, T. Polymer 1979, 20, 1804-1412
17. Hirotsu, S. Adv. Polym. Sci. 1993, 110, 2-26
18. Pelton, R. H.; Chibante, P. Coll Surf 1986, 20, 247-256
19. Pelton, R. Adv Coll Polym Int Sci 2000, 85, 1-31
20. Pelton, R. Macromol Symp 2004, 207, 57-66
21. Wu, X.; Pelton, R. H.; Hamielec, A. E.; Woods, D. R.; McPhee, W. Coll Polym Sci 1994, 272, 467-477
22. Varga, I.; Gilanyi. T.; Meszaros, R.; Filipsei, G.; Zrinyi, M. J Phys Chem B 2001, 105, 9071-9076
23. Kratz, K.; Hellweg, T.; Eimer, W.; Polymer 2001, 42, 6631-6639
24. Daly, E.; Saunders, B. R. Langmuir 2000, 16, 5546-5552
25. Mason, T.G.; Lin M.Y. Phys Rev E Stat Nonlin Soft Matter Phys. 2005, 71 (4 Pt 1), 040801 (Electronic publication 18.4.2005)
26. Seelenmeyer, S.; Deike, I.; Rosenfeldt, S.; Norhausen, Ch.; Dingenouts, N.; Ballauff, M.; Narayanan, T.; Lindner, P. J Chem Phys 2001, 114, 10471-10478

27. Arleth, L.; Xia, X.; Hjelm, R. P.; Wu, J.; Hu, Z. J Polym Sci B Polym Phys 2005, 43, 849-860
28. Woodward, N. C.; Chowdhry, B. Z.; Snowden, M. J.; Leharne, S. A.; Griffiths, P. C.; Winnington, A. L. Langmuir 2003, 19, 3202-3211
29. Guillermo, A.; Cohen Addad, J. P.; Bazile, J. P.; Duracher, D.; Elaissari, A.; Pichot, C. J Polym Sci B Polym Phys 2000, 38, 889-898
30. Zhu, P.W.; Napper, D.H. J Coll Int Sci 1994, 164, 489-494
31. Zhu, P. W.; Napper, D. H. Coll Surf A 1996, 113, 145-153
32. Shan, J.; Chen, J.;, Nuopponen; M.; Tenhu, H, Langmuir 2004, 20, 4671 -4676
33. Schönhoff, M.; Larsson, A.; Welzel, P.B.; Kuckling, D J Phys Chem B 2002, 106, 7800
34. Dingenouts, N.; Norhausen, C.; Ballauff, M. Macromolecules 1998, 31, 8912-8917
35. Kim, J.H.; Ballauff, M. Coll Polym Sci 1999, 277, 1210-1214
36. Dingenouts, N.; Seelenmeyer, S.; Deike, I.; Rosenfeldt, S.; Ballauff, M.; Lindner, P.; Narayanan, T. Phys Chem Chem Phys 2001, 3, 1169 -1174
37. Senff, H.; Richtering, W.; Norhausen, Ch.; Weiss, A.; Ballauff, M. Langmuir 1999, 15, 102-106
38. Bae, Y.H.; Jacobs, H.; Kim, S.W. J. Control. Release 1990, 11, 255-265
39. Yoshida, R.; Kaneko, Y.; Sakai, K.; Okano, T.; Sakurai, Y.; Bae, Y.H.; Kim, S.W. J. Control. Release 1994, 32, 79-102
40. Gutowska, A.; Bae, Y.H.; Feijen, J.; Kim, S.W. J. Control. Release 1992, 22, 95-104
41. Gutowska, A.; Bark, J.S.; Kwon, I.C.; Bae, Y.H.; Cha, Y.; Kim, S.W. J. Control. Release 1997, 48, 141-148
42. Lowe, T.L.; Virtanen, J.; Tenhu, H. Langmuir 1999, 15, 4259-4265.
43. Hoffman, C.; Schönhoff, M. Coll. Polym. Sci. 2009, 287, 1369-1376
44. Cole, M.A.; Voelcker, N.H.; Thissen, H.; Griesser, H.J. Biomaterials 2009, 30,1827-1850
45. Ho, K.M.; Li W.Y.; Wong C.H.; Li P. Coll Polym Sci 2010, 288, 1503-1523
46. Saunders, B.R.; Laajam, N.; Daly, E.; Teow, S.; Hu, X.; Stepto, R. Adv Coll Polym Sci 2009, 147-148, 251-261
47. Koskelainen, A.; Ala-Laurila, P.; Fyhrquist, N.; Donner, K. Nature 2000, 403:6766, 220-223
48. Arshavsky, V.Y.; Lamb, T.D.; Pugh Jr., E.N. Annu. Rev. Physiol. 2002, 64, 153-187
49. Brackett, L.; Shamim, M.T.; Daly, J.W. Biochem. Pharmacol. 1990, 39:12, 1897-1904
50. Saha, R.N.; Sajeev, C.; Sahoo, J.; Drug Delivery 2001, 8:3, 149-154
51. Roshdy, M.N.; Schnaare, R.L.; Schwartz, J.B. Pharmaceutical Development and Technology 2001, 6:4, 583-593
52. Miyazaki, S.; Kawasaki, N.; Endo, K.; Atwood, D. J. Pharm. Pharmacol. 2001, 53:9, 1185-1191
53. Freichel, O.L.; Lippold, B.C. Eur. J. Pharm. Biopharm. 2000, 50:3, 345-351
54. Zhang, F.; McGinity, J.W. Drug Development and Industrial Pharmacy 2000, 26:9, 931-942
55. Tsai, Y.L.; Jong, C.C.; Chen, H. J. Microencapsulation 2001, 18:6, 701-711

56. Lee, S.J.; Rosenberg, M. J. Control. Release 1999, 61, 123-136
57. De Sarro, A.; Grasso, S.; Zappala, M.; Nava, F.; De Sarro, G. Naynyn-Schmiedeberg's Arch Pharmacol 1997, 356, 48-55
58. Griffiths, P. C.; Stillbs, P.; Chowdry, B. Z.; Snowden, M. J. Coll Polym Sci 1995, 273, 405-411
59. Ohta, H.; Ando, I.; Fujishige, S.; Kubota, K. J Polym Sci B Polym Phys 1991, 29, 963-968
60. Tokuhiro, T.; Amiya, T.; Mamada, A.; Tanaka, T.; Macromolecules 1991, 24, 2936-2943
61. Zeng, F.; Tong, Z.; Feng, H. Polymer 1997, 38, 5539-5544
62. Desmukh, M. V.; Vaidya, A. A.; Kulkarni, M. G.; Rajamonahan, P. R.; Ganapathy, S. Polymer 2000, 41, 7951-7960
63. Durand, A.; Hourdet, D.; Lafuma, S. J Phys Chem B 2000, 104, 9371-9377
64. Spevacek, J.; Geschke, D.; Ilavsky, M. Polymer 2001, 42, 463-468
65. Spevacek, J.; Hanykova, L.; Ilavsky, M. Macromol Chem Phys 2001, 202, 1122-1129
66. Spevacek, J.; Hanykova, L.; Starovoytova, L. Macromolecules 2004, 37, 7710-7718
67. Starovoytova, L.; Spevacek, J.; Hanykova, L.; Ilavsky, M. Polymer 2004, 45, 5905-5911
68. Hanykova, L.; Spevacek, J.; Ilavsky, M. Polymer 2001, 42, 8607-8612
68. Starovoytova, L.; Spevacek, J.; Ilavsky, M. Polymer 2005, 46, 677-683
70. Spevacek, J. Curr. Op. Coll. Int. Sci. 2009, 14, 184-191
71. McPhee, W.; Tam, K.C.; Pelton, R.H. J Coll Int Sci 1993, 156, 24-30
72. Crowther, H.M.; Vincent, B. Coll Polym Sci 1998, 76, 46-51
73. Senff, H.; Richtering, W. Coll Polym Sci 2000, 278, 830 -840
74. Hellweg, T.; Dewhurst, C.D.; Bruckner, E.; Kratz, K.; Eimer, W. Coll Polym Sci 2000, 278, 972-978
75. Meyer, S; Richtering, W. Macromolecules 2000, 38, 1517-1519
76. Berndt, I.; Pedersen, J.S.; Lindner, P.; Richtering, W. Langmuir 2006, 22,459-468
77. Hyder Ali, A.; Srinivasan, S.V., J.M.S –Pure Appl. Chem. 1995, A32:12, 1985-1995
78. Laukkanen, A.; Hietala, S.; Maunu, S.L.; Tenhu, H. Macromolecules 2000, 33, 8703-8708
79. Mollica Jr., J.A.; Connors, K.A.; J. Am. Chem. Soc.1967, 89:2, 308-317
80. Connors, K.A.; Infeld, M.H.; Kline, B.J. J. Am. Chem. Soc.1969, 91:13, 3597-3603
81. Kramer, P.A.; Connors, K.A. J. Am. Chem. Soc. 1969, 91:10, 2600-2609
82. Stelmach, H.; Connors, K.A. J. Am. Chem. Soc. 1970, 92:4, 863-866
83. Stern, J.H.; Devore, J.A.; Hansen, S.L.; Yavuz, O. J. Phys. Chem. 1974, 78:19, 1922-1923
84. Yanuka, Y.; Zahalka, J.; Donbrow, M. J. Chem. Soc. Perkin Trans. 2 1986, 911-915
85. Segot-Chicq, S.; Peppas, N.A. J. Control. Release 1986, 3, 193-204
86. Makino, K.; Hiyoshi, J.; Hiroyuki, O. Coll. Surf. B: Biointerfaces 2001,20, 341-346
87. Daly, E.; Saunders, B. R. Phys Chem Chem Phys 2000, 2, 3187-3193

88. Woodward, N. C.; Chowdhry, B. Z.; Leharne, S. A.; Snowden, M. J. Eur Polym J 2000, 36, 1355-1364
89. Ding, Y.; Ye, X.;Zhang, G. Macromolecules 2005, 38, 904-908
90. Grinberg, N.V.; Dubovik, A.S.; Grinberg, V.Y.; Kuznetsov, D.V.; Makhaeva, E.E.; Grosberg, A.Y.; Tanaka, T. Macromolecules 1999, 32,1471-1475
91. Nemethy, G.; Sheraga, H.A.; J Chem Phys 1964, 41, 680-690
92. Wang, X.; Wu, C. Macromolecules 1999, 32, 4299-4301
93. Kujawa, P.; Winnik, F.M. Macromolecules 2001, 34, 4130-4135
94. Larsson, A.; Kuckling, D.; Schönhoff, M. Coll. Surf. A 2001, 190, 185 -192
95. Vihola, H. Academic Dissertation 2007, University of Helsinki, Faculty of Pharmacy